

## Theoretical spin-polarization parameters of molecular photoelectrons: Application to hydrogen halides

G. Rašeev, F. Keller, and H. Lefebvre-Brion

*Laboratoire de Photophysique Moléculaire, Bâtiment 213, Université de Paris-Sud, 91405 Orsay, France*

(Received 8 April 1987)

The nonrelativistic formulation of Cherepkov [J. Phys. B **14**, 2165 (1981)] of the spin-resolved photoionization cross sections is extended from the Hund's coupling case (a) to case (c) for the description of the ion molecular state. The spin-polarization parameters are analyzed in terms of a generalization of the partitioning scheme developed by Thiel [Chem. Phys. **77**, 103 (1983)] for the study of the  $\beta$  asymmetry parameter. This scheme allows a detailed analysis of different  $l$  contributions to spin-polarization parameters and, in the case of a single predominant term, a straightforward evaluation of these parameters. In the framework of the frozen-core static-exchange approximation, this formulation is used for the calculation and the interpretation of the spin-polarization parameters in the case of the  $\pi np$  outer-shell and  $d$  inner-shell photoionizations of the HBr and HI molecules in the energy region of Cooper minima and shape resonances.

### I. INTRODUCTION

The first molecular spin-polarization measurements were performed in 1980, on CO<sub>2</sub> and N<sub>2</sub>O.<sup>1</sup> More recently, halogens (I<sub>2</sub>, Br<sub>2</sub>) and methyl halides CH<sub>3</sub>Br and CH<sub>3</sub>I have been studied.<sup>2,3</sup> In 1981, Cherepkov<sup>4</sup> derived, in the framework of a general nonrelativistic theory, the spin-polarization parameters for diatomic molecules. Up to now, this formalism has been applied only to calculate the  $A$  and  $\xi$  spin-polarization parameters for the photoionization of HI,<sup>5</sup> in the spin-orbit autoionization region between the two <sup>2</sup> $\Pi$  thresholds of the ion ground state.

Since 1969,<sup>6</sup> photoelectron spin-polarization measurements and *ab initio* calculations have allowed a better understanding of the influence of the spin-orbit interaction on the atomic photoionization process. A detailed review of the contributions devoted to atomic and molecular photoelectron spin polarization was written by Cherepkov<sup>7</sup> in 1983. For closed-shell atoms, such as rare gases<sup>8-11</sup> and mercury,<sup>12-14</sup> experiment and the results of relativistic and nonrelativistic<sup>10</sup> theories can be compared. For atoms with atomic number  $Z \leq 54$ , it appears<sup>16</sup> that nonrelativistic theories predict reasonable values for the spin-polarization parameters for subshells with orbital angular momentum  $l > 0$ .

The main difference between atoms and molecules comes from the nonspherical molecular field which removes the energy degeneracy between substates of different quantum numbers  $\lambda$ . ( $\lambda$  is the projection on the internuclear axis of the electronic orbital angular momentum  $l$ .) This loss of symmetry increases the number of theoretical quantities (such as, e.g., transition moments) which describe the photoionization process.

In this paper, we extend Cherepkov's formalism in two directions: we take into account the mixing between different  $l$  generated by the molecular field, and we describe the ionic molecular state either as Hund's coupling scheme (a) or (c). We generalize, to the spin-polarization parameters  $A$  (denoted  $\bar{P}$  in this paper),  $\xi$ ,

and  $\gamma$ , the partitioning scheme introduced by Thiel<sup>17</sup> for the photoelectron angular-distribution asymmetry parameter  $\beta$ . This allows us to analyze the different atomic and molecular contributions to the spin-polarization parameters.

We have applied the above method to the *ab initio* study of the photoionization of the inner  $3d$  and  $4d$ , and outer  $\pi 4p$  and  $\pi 5p$  subshells of HBr and HI. These hydrogen halides are compared with the well-known isoelectronic Kr and Xe atoms. This allows us to discuss our spin-polarization results in terms of atomic and molecular contributions.

In Sec. II, we review the theoretical approach leading to the polarization parameters. In Sec. III we present the results of our calculations and we compare them to available atomic and molecular experimental data.

### II. THEORETICAL APPROACH

In this section we summarize the theoretical framework of our approach. Let us first highlight the major points. The key expression is the spin-resolved differential cross section [Eq. (1)]. For general discussion and a link with atomic formulas, we expand in (5) the  $\mathbf{P}$  polarization vector appearing in (1) in terms of spin-up and -down laboratory-frame transition moments. Usually Eq. (1) is expressed in terms of five parameters  $\sigma$ ,  $\beta$ ,  $\bar{P}$ ,  $\gamma$ , and  $\xi$  [Eq. (6)]. There are these parameters which are calculated theoretically and measured experimentally. Particularly important are Eqs. (15)–(17) which establish expressions of the spin-polarization parameters in a very simple form of a product of a geometrical factor which is energy independent and an energy-dependent dynamical factor. The present formulation allows us also to separate the contributions of different asymptotic or molecular channels of the final state to differential cross-section parameters. This is known as the partitioning scheme. In Eqs. (18) and (19) we give the expressions of parameters summed over all asymptotic channels. They are similar to the expressions derived by Cherepkov.<sup>4</sup> Tables III and IV contain the numerical

values of the geometrical factors for easy reference and direct estimation of parameters in the case of a single dominant term. The section ends with some examples and with the relations between parameters in the Hund's case (a) and (c).

**A. Summary of the nonrelativistic formalism of Cherepkov (Ref. 4); extension of the partitioning scheme of Thiel (Ref. 13) to spin-polarization parameters**

The  $Z$  axis of the laboratory coordinate system (Fig. 1) is defined using the photon properties (direction of propagation, spin, or vector of the electric field). The angle between the direction of propagation  $\mathbf{k}$  of the electron ejected from the molecule and the  $Z$  axis is  $\theta_k$  and the three components of the electron spin-polarization vector  $\mathbf{P}_{\Lambda^+\Omega^+}$  are  $P_{\Lambda^+\Omega^+}^X(\theta_k)$ ,  $P_{\Lambda^+\Omega^+}^Y(\theta_k)$ , and  $P_{\Lambda^+\Omega^+}^Z(\theta_k)$ . The angles of  $\mathbf{P}_{\Lambda^+\Omega^+}$  with respect to the coordinate system are  $\theta_p$  and  $\phi_p$ . Following Cherepkov,<sup>4</sup> Heckenkamp *et al.*,<sup>18</sup> and Huang<sup>15</sup> [Eq. (4.1)], the differential photoionization cross section of a molecule for the ejection of the photoelectron into a given infinitesimal solid angle with a spin polarization  $\mathbf{P}_{\Lambda^+\Omega^+}$  can be written in the following form:

$$\begin{aligned} \sigma_{\Lambda^+\Omega^+}^{\text{diff}} = C_E \text{Tr}(\rho T T^*) = \frac{\sigma_{\Lambda^+\Omega^+}}{8\pi} F_{\Lambda^+\Omega^+}(\beta, \theta_k) [1 + \cos\theta_p P_{\Lambda^+\Omega^+}^Z(\theta_k) + \sin\theta_p \cos\phi_p P_{\Lambda^+\Omega^+}^X(\theta_k) \\ + \sin\theta_p \sin\phi_p P_{\Lambda^+\Omega^+}^Y(\theta_k)] . \end{aligned} \quad (1)$$

In (1)  $\rho$  is the photon spin-density matrix defined by Huang<sup>15</sup> (Eqs. 2.1 and 4.1),

$$\rho = \frac{1}{2} \begin{bmatrix} 1 + \cos\theta_p & \sin\theta_p \exp(-i\phi_p) \\ \sin\theta_p \exp(i\phi_p) & 1 - \cos\theta_p \end{bmatrix} ,$$

and  $T$  is the transition moment defined as a column vector with the components  $T_\alpha$  and  $T_\beta$  for the spin projection  $\mu$  of the photoelectron.  $F_{\Lambda^+\Omega^+}$  is proportional to the differential spin-unresolved cross section. Note that the angular-distribution asymmetry parameter  $\beta$  appearing in  $F_{\Lambda^+\Omega^+}$  is not to be confused with the subscript  $\beta$  of the transition moment defined above [see also Eq. (5)].

$$\begin{aligned} \Psi_{\Lambda^+\Omega^+,\mu}^{(-)}(\mathbf{k}, \mathbf{r}) &= \sum_{l_1 m} \frac{1}{2i} i^{l_1} \exp[-i\eta_{l_1}] \psi_{\Lambda^+\Omega^+,l_1 m}^{(-)}(k, \mathbf{r}) \chi_\mu Y_{l_1 m}(\hat{\mathbf{k}}) \\ &= \sum_{l_1 m} \frac{1}{2i} i^{l_1} \exp[-i\eta_{l_1}] \sum_{l_2} \phi_{\Lambda^+\Omega^+,l_2 m,l_1 m}^{(-)}(k, r) \chi_\mu Y_{l_1 m}(\hat{\mathbf{k}}) Y_{l_2 m}(\hat{\mathbf{r}}) . \end{aligned} \quad (2)$$

In (2)  $\mathbf{k}$  and  $\mathbf{r}$  are defined in the laboratory frame,  $l$  is the electron angular momentum, and  $m$  and  $\mu$  are the projections of the angular and spin momentum of the ejected electron onto the  $Z$  laboratory axis. The wave func-

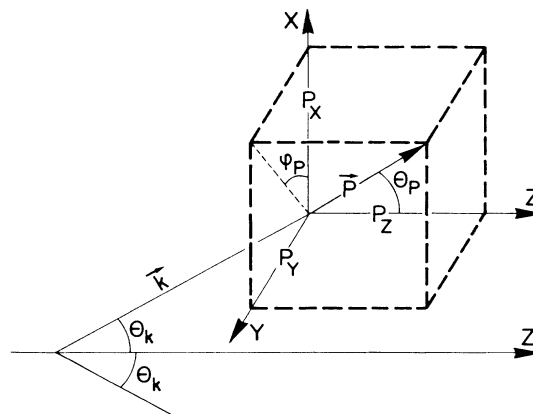


FIG. 1. Laboratory coordinate system. In this coordinate system,  $Z$  axis is in the direction of photon spin for circularly polarized photon ( $s_r$ ), or of electric vector  $\mathbf{e}$  for linearly polarized light, or of the light propagation  $\mathbf{k}_r$  for unpolarized light.  $\mathbf{k}$ ,  $\mathbf{P}$ , and  $\theta_k$  are the linear momentum, polarization, and ejection angle of the electron. The angles  $\theta_p$  and  $\phi_p$  define the orientation of the polarization in the laboratory frame and the reaction plane is defined by direction of  $Z$  and  $\mathbf{k}$ .

$C_E$  is a constant detailed in Eqs. (5) and (6) below. The subscripts  $\Lambda^+$  and  $\Omega^+$  are the projections onto the internuclear axis of the electronic orbital and electronic plus spin angular momenta of the final ionic state (omitted in the following whenever no ambiguity is possible),  $\sigma_{\Lambda^+\Omega^+}^{\text{diff}}$  and  $\sigma_{\Lambda^+\Omega^+}$  are differential and integrated cross sections.

We now establish a relation between the laboratory-frame transition moment [Eq. (3a) below] and the polarization vector  $\mathbf{P}$  appearing in (1). We start by introducing the final-state continuum molecular wave function in laboratory frame (see, e.g., Fano and Dill,<sup>19</sup> Dill and Dehmer<sup>20</sup> [Eqs. (39) and (41)], and Tully *et al.*<sup>21</sup> [Eqs. (2.12) and (2.13)]):

tions  $\Psi_{\Lambda^+\Omega^+,\mu}^{(-)}$ ,  $\psi_{\Lambda^+\Omega^+,l_1 m}^{(-)}$ , and  $\phi_{\Lambda^+\Omega^+,l_1 m,l_2 m}^{(-)}$  characterize the  $N$ -electron final state, and  $\eta_{l_1}$  is the Coulomb phase shift. The spin function  $\chi_\mu$  is that of the ejected electron in the laboratory frame. Compared with Eqs.

(2) and (3) of Cherepkov<sup>4</sup> the present Eq. (2) contains a double summation over  $l_1, m$  and  $l_2, m$  instead of a simple summation in Cherepkov's formulation. The second summation appears as a consequence of the nonspherical nature of the molecular potential. The dipole transition moment from an initial state  $\Psi^{\Lambda''}$  to a final state  $\Psi_{\Lambda^+\Omega^+, \mu}^{(-)}$  defined in (2) can be written as

$$T_{\Lambda^+\Omega^+, \mu}^{(-)m^{\text{ph}}, \Lambda''}(\mathbf{k}) = \sum_{l, m} Y_{lm}(\hat{\mathbf{k}}) i^l \exp(-i\eta_l) T_{\Lambda^+\Omega^+, lm\mu}^{(-)m^{\text{ph}}, \Lambda''}(k), \quad (3a)$$

where

$$T_{\Lambda^+\Omega^+, lm\mu}^{(-)m^{\text{ph}}, \Lambda''}(k) = \frac{1}{2i} \left[ \frac{4\pi}{3} \right]^{1/2} \times \left\langle \psi_{\Lambda^+\Omega^+, lm}^{(-)}(k, \mathbf{r}) \chi_{\mu} | r Y_{lm}^{\text{ph}}(\hat{\mathbf{r}}) | \Psi^{\Lambda''} \right\rangle. \quad (3b)$$

In (3)  $m^{\text{ph}}$  is the projection of the photon spin-angular momentum on the  $Z$  laboratory axis. We have the absolutely equivalent form of (2) and (3) in the molecular frame if we replace projections  $m^{\text{ph}}, m$ , and  $\mu$  and vectors  $\mathbf{k}$  and  $\mathbf{r}$  in the laboratory frame by projections  $m^{\gamma}, \lambda$ , and  $\mu'$  and vectors  $\mathbf{k}'$  and  $\mathbf{r}'$  in the molecular frame. The transformation between the two functions is made through rotational matrices (see, e.g., Cherepkov<sup>4</sup> and Rose<sup>22</sup>).

Now  $T_{\Lambda^+\Omega^+, \mu}^{(-)m^{\text{ph}}, \Lambda''}(\mathbf{k})$  is a complex number and can be written in polar form as

$$T_{\Lambda^+\Omega^+, \mu}^{(-)m^{\text{ph}}, \Lambda''}(\mathbf{k}) = |T_{\Lambda^+\Omega^+, \mu}^{(-)m^{\text{ph}}, \Lambda''}(\mathbf{k})| \exp[i\delta_{\Lambda^+\Omega^+, \mu}^{m^{\text{ph}}, \Lambda''}(\mathbf{k})]. \quad (4)$$

The transition moment (4) represents one of the components of spin  $\alpha$  or  $\beta$  of the column-vector transition moment  $T$  introduced in (1). Replacing this column vector in (1) we can identify the different components  $P^Z, P^X$ , and  $P^Y$  of the electron spin-polarization vector  $\mathbf{P}$  (neglecting the subscript  $\Lambda^+\Omega^+$  and the superscripts  $m^{\text{ph}}, \Lambda''$ ),

$$F(\beta, \theta_k) = \frac{|T_{\alpha}(\mathbf{k})|^2 + |T_{\beta}(\mathbf{k})|^2}{\sigma/C_E}, \quad (5a)$$

$$P^Z(\theta_k) = \frac{|T_{\alpha}(\mathbf{k})|^2 - |T_{\beta}(\mathbf{k})|^2}{F(\beta, \theta_k)\sigma/C_E}, \quad (5b)$$

$$P^X(\theta_k) = \frac{|T_{\alpha}(\mathbf{k})| |T_{\beta}(\mathbf{k})| \cos(\delta_{\alpha} - \delta_{\beta})}{F(\beta, \theta_k)\sigma/C_E}, \quad (5c)$$

$$P^Y(\theta_k) = \frac{|T_{\alpha}(\mathbf{k})| |T_{\beta}(\mathbf{k})| \sin(\delta_{\alpha} - \delta_{\beta})}{F(\beta, \theta_k)\sigma/C_E}, \quad (5d)$$

where  $C_E = (4\pi^2 e^2 / 3\hbar c) \Delta E$  is the usual energy-dependent constant appearing in the cross section and  $\Delta E$  is the difference between the initial- and final-state energies (i.e., the photon energy) and  $e, \hbar$ , and  $c$  are the electron charge, Planck's constant, and the velocity of light. In (5) the polarization  $\mathbf{P}$  gives the probability to

find the spin of the photoelectron oriented in a given direction. The transition moments  $T_{\alpha}$  and  $T_{\beta}$  (calculated in laboratory frame) correspond to the separate probability to reach the spin  $\alpha$  or  $\beta$  components of the final-state wave function of the photoelectron from the initial one. Equations (5) establish a link between these quantities.

Now let us rewrite (5) in terms of the polarization parameters  $\bar{P}, \gamma$ , and  $\xi$  [we reintroduce here the subscript  $\Lambda^+\Omega^+$  to connect (6) to relations (18c) and (19)],

$$F_{\Lambda^+\Omega^+}(\beta, \theta_k) = 1 + c\beta_{\Lambda^+\Omega^+} P_2(\cos\theta_k), \quad (6a)$$

$$P_{\Lambda^+\Omega^+}^Z(\theta_k) = c' \frac{\bar{P}_{\Lambda^+\Omega^+} - \gamma_{\Lambda^+\Omega^+} P_2(\cos\theta_k)}{F_{\Lambda^+\Omega^+}(\beta, \theta_k)}, \quad (6b)$$

$$P_{\Lambda^+\Omega^+}^X(\theta_k) = -\frac{c' \gamma_{\Lambda^+\Omega^+} P_2^1(\cos\theta_k)}{2 F_{\Lambda^+\Omega^+}(\beta, \theta_k)} = -\frac{3c' \gamma_{\Lambda^+\Omega^+} \cos\theta_k \sin\theta_k}{2 F_{\Lambda^+\Omega^+}(\beta, \theta_k)}, \quad (6c)$$

$$P_{\Lambda^+\Omega^+}^Y(\theta_k) = -\frac{4c \xi_{\Lambda^+\Omega^+} P_2^1(\cos\theta_k)}{3 F_{\Lambda^+\Omega^+}(\beta, \theta_k)} = -4c \frac{\xi_{\Lambda^+\Omega^+} \cos\theta_k \sin\theta_k}{F_{\Lambda^+\Omega^+}(\beta, \theta_k)}. \quad (6d)$$

In (6)  $\beta_{\Lambda^+\Omega^+}$  is the asymmetry parameter and  $\bar{P}_{\Lambda^+\Omega^+}, \gamma_{\Lambda^+\Omega^+}$ , and  $\xi_{\Lambda^+\Omega^+}$  are spin-polarization parameters.  $P_2(\cos\theta_k)$  and  $P_2^1(\cos\theta_k)$  are, respectively, the second Legendre polynomial and the associated Legendre function. The constants  $c$  and  $c'$  depend on the polarization of the light and its helicity:  $c$  equals 1 for linearly polarized light and  $-\frac{1}{2}$  for circularly and unpolarized light whereas  $c'$  equals  $\pm 1$  for circularly polarized light depending on the helicity and zero for linearly and unpolarized light (i.e.,  $P^X$  and  $P^Z$  are zero). Therefore  $\bar{P}$ , the term independent of the electron ejection angle, is nonzero only for circularly polarized light. For circularly polarized light, the angular behavior with respect to  $\theta_k$  is such that at the magic angle where  $P_2(\cos\theta_k)$  is zero, the differential cross section without spin yields the total cross section  $\sigma_{\Lambda^+\Omega^+}$  and the two measured spin-polarization components  $P^Z$  and  $P^Y$  are proportional, respectively, to  $\bar{P}$  and  $\xi$ . We should also mention the formulas for elliptically polarized light given by Heckenkamp *et al.*<sup>18</sup>

Various authors have used different notations<sup>4,5,7,11,18,23,24</sup> for the spin-polarization parameters  $\bar{P}, \gamma$ , and  $\xi$  introduced in (6). We present in Table I the correspondences between these notations. In the first column we give the notations used in the present paper. We have chosen one of the most widely used notations except in the case of the average polarization  $\bar{P}$ . The usual notation for averaged polarization is  $A$  but in molecules it can be confused with the spin-orbit coupling constant  $A$  of the ion state. The notation  $\bar{P}$  has been chosen since it has already been used in the book of Kessler<sup>25</sup> and this notation contains some information

TABLE I. Relations between polarization parameters introduced by several authors.

This work	Lefebvre-Brion <i>et al.</i> <sup>a</sup>	Heckenkamp <i>et al.</i> <sup>b</sup>	Cherepkov <sup>c</sup>	Cherepkov <sup>d</sup>	Lee <sup>e</sup>	Huang <i>et al.</i> <sup>f</sup>
$\bar{P}$	$A$	$A$	$A$	$A$	$\frac{1}{2}(\gamma + 2\delta)$	$\delta$
$\gamma$		$\alpha$	$\gamma$	$\gamma$	$-\frac{2}{3}(\gamma - \delta)$	$-\frac{2}{3}(\xi + \xi)$
$\xi$	$-\xi$	$\xi$	$-\xi$	$\eta/2$	$\xi$	$\eta/2$

<sup>a</sup>Reference 5.

<sup>b</sup>Reference 18.

<sup>c</sup>Reference 24. The expression of  $\gamma$  in this paper is incorrect.

<sup>d</sup>References 4 and 7.

<sup>e</sup>Reference 23.

<sup>f</sup>Reference 11.

about its physical meaning.

The formulas (6) are formally the same as the atomic formulas of the photoelectron spin-polarized cross section. The difference appears in the detailed expressions of polarization parameters and in the definition of two nonequivalent molecular and laboratory frames. The laboratory frame is as in atoms defined by photon characteristics. The molecular frame has no definite orientation since in gas phase the molecules are randomly oriented. This is translated in the formulation by averaging over the molecular-frame orientation. Simple interpretation of the parameters is given if we compare Eqs. (6) and (5). The  $P^Z$  parameter contains  $\bar{P}$  and  $\gamma$  and corresponds to the square difference of spin-up and -down transition moments of Eq. (4). It can be written as  $\bar{P}[1 - (\gamma/\bar{P})P_2(\cos\theta_k)]$  which shows the similarity with the spin-unresolved differential cross section and consequently between  $\bar{P}$  and  $\sigma$  and  $\gamma/\bar{P}$  and  $\beta$ .  $P^X$  and  $P^Y$  contain information concerning the difference of phases between laboratory transition moments with spins up and down.

In the following, we write explicitly the polarization parameters of Eq. (6) transforming the formulas (2)–(4) to the molecular frame and averaging over the arbitrary orientation of the target. In the molecular frame the  $z$  axis corresponds to the internuclear axis of diatomic molecules. The transition moment has the form

$$T_{\Lambda^+\Omega^+,l\lambda\mu'}^{(-)m\gamma,\Lambda''}(k) = \frac{1}{2i} \left[ \frac{4\pi}{3} \right]^{1/2} \langle \psi_{\Lambda^+\Omega^+,l\lambda}^{(-)}(k, \mathbf{r}') \chi_{\mu'} | r' Y_{1m\gamma}(\hat{\mathbf{r}}') | \psi^{\Lambda''} \rangle. \quad (7)$$

As mentioned above this transition moment is related to (3b) by a transformation from the laboratory to the molecular frame using the rotational matrices<sup>22</sup> as detailed by Cherepkov.<sup>4</sup> In the Cherepkov's formalism, as in any differential cross-section formalism, the derivation concerns transition moments (i.e., integrated over  $r$  quantities) where the second summation over  $l$  appearing in (2) is hidden. In other words, how these short-range quantities are calculated has no influence on the formalism which essentially treats the asymptotic behavior of the electrons. Therefore Eq. (7) is formally equivalent to

Eq. (7) of Cherepkov.<sup>4</sup> Consequently, Cherepkov's formalism is still valid when molecular  $l$  mixing is introduced as in Eqs. (2), (3), and (7). It is also interesting to mention that if the initial and final states are not one configuration states the transition moment can be written in terms of a first-order density matrix as defined by Lowdin<sup>26</sup> times a one-electron transition moment as detailed in Eqs. (42) and (43) of Raşeev and Le Rouzo.<sup>27</sup> This more complicated form of the moment will not change the formalism of Cherepkov.<sup>4</sup>

Now we turn to the use of the partitioning scheme of Thiel<sup>17</sup> for the polarization of the spin of the photoelectron. This scheme is interesting since we can separate the contribution of different  $l$  to a given polarization parameter and therefore we can single out the main contributions and interpret their physical meaning. Following Fano and Dill<sup>19</sup> and Thiel<sup>17</sup> we split the cross section into a dynamical factor introduced in Eq. (9) below and a geometrical factor defined in Eqs. (13) and (14). This separation is not only formal. The dynamical factor has to be calculated at each photon energy whereas the geometrical factor is an energy-independent quantity depending on the number and type of channels considered in the calculation.

To obtain the dynamical part we start from the transition moment (7) in the molecular frame. It is a complex quantity which can be rewritten in polar form as

$$T_{\Lambda^+\Omega^+,l\lambda\mu'}^{(-)m\gamma,\Lambda''}(k) = |T_{\Lambda^+\Omega^+,l\lambda\mu'}^{(-)m\gamma,\Lambda''}(k)| \exp[i\delta_{\Lambda^+\Omega^+,l\lambda\mu'}^{m\gamma,\Lambda''}(k)]. \quad (8)$$

In (8)  $\delta_{\Lambda^+\Omega^+,l\lambda\mu'}^{m\gamma,\Lambda''}(k)$  is the argument of the complex number. Using this transition moment, we write the dynamical factor of the cross section as

$$D_{\Lambda^+\Omega^+,\mu'}^{l_1l_2,\lambda_1\lambda_2} = M_{\Lambda^+\Omega^+,\mu'}^{l_1l_2,\lambda_1\lambda_2} \exp(-i\Phi_{\Lambda^+\Omega^+,\mu'}^{l_1l_2,\lambda_1\lambda_2}). \quad (9)$$

The cosine part of (9) (noted in the following as  ${}_cD$ ) contributes to the  $\beta$  and  $\gamma$  parameters whereas the sine part (noted in the following as  ${}_sD$ ) contributes to  $\xi$ . In (9)  $M_{\Lambda^+\Omega^+,\mu'}^{l_1l_2,\lambda_1\lambda_2}$  represents the modulus of the product of two transition moments

$$M_{\Lambda^+\Omega^+,\mu'}^{l_1l_2,\lambda_1\lambda_2} = |T_{\Lambda^+\Omega^+,l_1\lambda_1\mu'}^{(-)m_1^{\gamma_1},\Lambda''}| |T_{\Lambda^+\Omega^+,l_2\lambda_2\mu'}^{(-)m_2^{\gamma_2},\Lambda''}| / B_{\Lambda^+\Omega^+}, \quad (10)$$

where  $B_{\Lambda^+\Omega^+}$  is given by

$$B_{\Lambda^+\Omega^+} = \sum_l \sum_{\lambda, m^\gamma, \mu'} |T_{\Lambda^+\Omega^+, l\lambda\mu'}^{(-)m^\gamma, \Lambda''}|^2 \quad (11)$$

and  $\Phi_{\Lambda^+\Omega^+, \mu'}^{l_1 l_2, \lambda_1 \lambda_2}$  is the difference of phases of the two transition moments,

$$\Phi_{\Lambda^+\Omega^+, \mu'}^{l_1 l_2, \lambda_1 \lambda_2} = (\eta_{l_1} - \eta_{l_2}) + \delta_{\Lambda^+\Omega^+, l_1 \lambda_1 \mu'}^{m_1^\gamma, \Lambda''} - \delta_{\Lambda^+\Omega^+, l_2 \lambda_2 \mu'}^{m_2^\gamma, \Lambda''}, \quad (12)$$

where the difference between Coulomb phases is given by

$$\eta_{l_1} - \eta_{l_2} = - \sum_{j=0}^{l_1 - l_2} \tan^{-1} \frac{1}{k(l_2 + j)}, \quad (12')$$

where  $l_1 - l_2 > 0$  and  $k$  is the momentum of the electron. In the left-hand side of Eqs. (10), (11), and (14) below, we have omitted  $m^\gamma$  and  $\Lambda''$  as superscripts. This is possible as we have the selection rule  $\Lambda'' + m^\gamma = \Lambda^+ + \lambda$  which fixes unequivocally  $m^\gamma$  when  $\Lambda^+$  and  $\lambda$  are given.  $\Lambda''$  of the initial state is well known and unique for all the final channels.

Following Thiel<sup>17</sup> the next step is to replace  $\lambda_1$  and  $\lambda_2$  by  $\alpha_1 = |\lambda_1|$  and  $\alpha_2 = |\lambda_2|$  in Eqs. (9)–(12). To perform this simplification, we rewrite (11) in the following form:

$$B_{\Lambda^+\Omega^+} = \sum_{l, \alpha, \mu'} (1 + \delta_{0, \Lambda^+} \delta_{l\alpha}) |T_{\Lambda^+\Omega^+, l\alpha\mu'}^{(-)m^\gamma, \Lambda''}|^2. \quad (11')$$

The geometrical factor contains the integration over the rotational matrices linking the molecular-frame transition moments (7) and the laboratory-frame transition moments of Eq. (3). It contains also the spherical harmonics  $Y_{lm}(\hat{\mathbf{k}})$  (see Cherepkov<sup>4,7</sup>). When averaged over the arbitrary orientations of molecules in the gas phase and modified to take into account the modulus of  $\lambda$  through the factor  ${}_a F$ , it takes the following form:

$$\begin{aligned} G_{\Lambda^+}^{l_1 l_2, \alpha_1 \alpha_2, m_1^\gamma m_2^\gamma} &= \sqrt{30} i^{l_1 + l_2} \sqrt{(2l_1 + 1)(2l_2 + 1)} {}_a F_{\Lambda^+}^{l_1 l_2, \alpha_1 \alpha_2} \\ &\times (-1)^{l_2 + \alpha_1 + m_1^\gamma} \\ &\times \begin{bmatrix} l_1 & l_2 & 2 \\ 0 & 0 & 0 \end{bmatrix} \begin{bmatrix} l_1 & l_2 & 2 \\ \alpha_1 & -\alpha_2 & m_2^\gamma - m_1^\gamma \end{bmatrix}, \quad (13) \end{aligned}$$

where  ${}_a F$  is similar to the factor introduced by Thiel<sup>17</sup> and for completeness is reproduced in Table II. Three geometrical factors are defined

$$\beta G_{\Lambda^+}^{l_1 l_2, \alpha_1 \alpha_2} = G_{\Lambda^+}^{l_1 l_2, \alpha_1 \alpha_2, m_1^\gamma m_2^\gamma} \begin{bmatrix} 1 & 1 & 2 \\ -m_1^\gamma & m_2^\gamma & m_1^\gamma - m_2^\gamma \end{bmatrix}, \quad (14a)$$

$$\xi G_{\Lambda^+\mu'}^{l_1 l_2, \alpha_1 \alpha_2} = -\frac{1}{8} (-1)^{\mu' - 1/2} (m_2^\gamma - m_1^\gamma) \beta G_{\Lambda^+}^{l_1 l_2, \alpha_1 \alpha_2}, \quad (14b)$$

TABLE II. Numerical values of the  ${}_a F$  factor in Eq. (13) for different symmetries. The initial state is assumed to be a  $\Sigma$  state.

$\Lambda^+$	$\alpha_1$	$\alpha_2$	${}_a F$
0	0	0	$2 - \delta_{l_1 l_2}$
0	0	1	4
0	1	0	4
0	1	1	$2(2 - \delta_{l_1 l_2})^a$
1,2,3	$\alpha_1$	$\alpha_2$	$2 - \delta_{l_1 l_2} \delta_{\alpha_1 \alpha_2}$

<sup>a</sup>For this term we have to take into account two contributions: one with  $\alpha_1 = \alpha_2 = 1$  and the other with  $\alpha_1 = -\alpha_2 = 1$ .

$$\begin{aligned} \gamma G_{\Lambda^+\mu'}^{l_1 l_2, \alpha_1 \alpha_2} &= -\frac{1}{\sqrt{20}} (-1)^{\mu' - 1/2} [4 - (m_1^\gamma - m_2^\gamma)^2]^{1/2} \\ &\times \begin{bmatrix} 1 & 1 & 1 \\ -m_1^\gamma & m_2^\gamma & m_1^\gamma - m_2^\gamma \end{bmatrix} \\ &\times G_{\Lambda^+}^{l_1 l_2, \alpha_1 \alpha_2, m_1^\gamma m_2^\gamma}. \quad (14c) \end{aligned}$$

Note that the geometrical factor of  $\bar{P}$  is so simple [see Eq. (19b) below] that we do not reproduce it here. Now the spin-polarization parameters defined in (6) can be rewritten using (9) and (14),

$$\beta_{\Lambda^+\Omega^+, \mu'}^{l_1 l_2, \alpha_1 \alpha_2} = \beta G_{\Lambda^+}^{l_1 l_2, \alpha_1 \alpha_2} {}_c D_{\Lambda^+\Omega^+, \mu'}^{l_1 l_2, \alpha_1 \alpha_2}, \quad (15)$$

$$\gamma_{\Lambda^+\Omega^+, \mu'}^{l_1 l_2, \alpha_1 \alpha_2} = \gamma G_{\Lambda^+\mu'}^{l_1 l_2, \alpha_1 \alpha_2} {}_c D_{\Lambda^+\Omega^+, \mu'}^{l_1 l_2, \alpha_1 \alpha_2}, \quad (16)$$

$$\xi_{\Lambda^+\Omega^+, \mu'}^{l_1 l_2, \alpha_1 \alpha_2} = i^2 \xi G_{\Lambda^+\mu'}^{l_1 l_2, \alpha_1 \alpha_2} {}_s D_{\Lambda^+\Omega^+, \mu'}^{l_1 l_2, \alpha_1 \alpha_2}. \quad (17)$$

In Eq. (17)  $i^2$  comes from the geometrical factor Eq. (14b) and the imaginary part of the exponential Eq. (9). As we define ratios  $\xi R$  in Sec. II B we prefer that  $\xi G$  be defined as a real number. We can now write the recombination formulas (18) for the  $\beta$  parameter

$$\beta_{\Lambda^+\Omega^+}^{l_1 l_2} = \sum_{\substack{\alpha_1, \alpha_2 \\ (\alpha_1 \geq \alpha_2)}} \sum_{\mu'} \beta_{\Lambda^+\Omega^+, \mu'}^{l_1 l_2, \alpha_1 \alpha_2}, \quad (18a)$$

$$\beta_{\Lambda^+\Omega^+}^{\alpha_1 \alpha_2} = \sum_{\substack{l_1, l_2 \\ (l_1 \geq l_2)}} \sum_{\mu'} \beta_{\Lambda^+\Omega^+, \mu'}^{l_1 l_2, \alpha_1 \alpha_2}, \quad (18b)$$

$$\beta_{\Lambda^+\Omega^+} = \sum_{\substack{l_1, l_2 \\ (l_1 \geq l_2)}} \beta_{\Lambda^+\Omega^+}^{l_1 l_2} = \sum_{\substack{\alpha_1, \alpha_2 \\ (\alpha_1 \geq \alpha_2)}} \beta_{\Lambda^+\Omega^+}^{\alpha_1 \alpha_2}. \quad (18c)$$

Similar relations are valid for  $\gamma$  and  $\xi$ . Finally, using (9) and (10) the total cross section and the average polarization can be written in the following form:

$$\begin{aligned} \sigma_{\Lambda^+\Omega^+} &= C_E \sum_{l, \lambda} \sum_{\mu'} M_{\Lambda^+\Omega^+, \mu'}^{ll, \lambda\lambda} \\ &= \sum_{l, \lambda} \sigma_{\Lambda^+\Omega^+}^{l\lambda} = \sum_{\lambda} \sigma_{\Lambda^+\Omega^+}^{\lambda} = \sum_l \sigma_{\Lambda^+\Omega^+}^l, \quad (19a) \end{aligned}$$

$$\begin{aligned}\bar{P}_{\Lambda^+\Omega^+} &= \sum_{l,\lambda} \sum_{\mu'} \frac{1}{2} (-1)^{\mu'-1/2} m^\gamma M_{\Lambda^+\Omega^+,\mu'}^{ll,\lambda\lambda} \\ &= \sum_{l,\lambda} \bar{P}_{\Lambda^+\Omega^+}^{l\lambda} = \sum_{\lambda} \bar{P}_{\Lambda^+\Omega^+}^\lambda = \sum_l \bar{P}_{\Lambda^+\Omega^+}^l,\end{aligned}\quad (19b)$$

where  $C_E$  is defined in connection with Eq. (5). In the case of doublet states the sum over  $\mu'$  in the above formulas reduces to only one term.

We have completed the generalization of the partitioning scheme of Thiel.<sup>17</sup> One of the advantages of this scheme is that it can establish a link between molecular- and laboratory-frame quantities. The label  $l$  in Eqs. (3b) and (7) is common to the two frames. The projection of the spin-polarization vector  $\mathbf{P}$  in the laboratory frame [Eqs. (5) and (6)] can therefore be written as  $P^X = \sum_{l_1, l_2} P^{X, l_1 l_2}$  (and similar expressions for  $P^Y$  and  $P^Z$ ) and an analysis can be done in terms of different  $l$  valid in the two frames. The expressions of spin-polarization parameters in terms of  $l_1 l_2$  [as, for example, Eq. (18a)] have to be preferred as they have a meaning in the laboratory frame which is the one where the experiment is performed. They are connected to the probabili-

ty that an electron exhibits a spin up or down as shown in relations (5) and through (6) to the spin- and angle-resolved differential cross section [Eq. (1)].

In the particular cases where either the atom (rare gases) or the remaining ion (alkaline metals) has closed shells, if the atom is in  $LS$  coupling and the five parameters introduced above are known from experiment, then we can derive backwards the transition moments and the phase factors from experiment. However, in molecules, due essentially to the  $l$  mixing, the number of transition moments is much larger and such a procedure is impossible without severe approximations. Nevertheless, using the partitioning scheme devised above, we can distinguish contributions of different  $l$  and  $\alpha$  to a given parameter [see Eqs. (18) and (19)]. As illustrated in Sec. II B, this scheme can also be used to separate atomic (in fact, mixed atomic and molecular) contributions which satisfy the atomic-transition selection rule  $\Delta l = \pm 1$  from the purely molecular one.

Finally, let us briefly discuss the case when there is no spin-orbit coupling in the continuum. Cherepkov<sup>4</sup> has given particular formulas valid for doublet ionic cores.

TABLE III. Diagonal terms of the geometrical factor  $\beta G_{\Lambda^+}^{ll,\alpha_1\alpha_2}$  and the ratios  ${}_\gamma R_{\mu'}^{m_1^\gamma m_2^\gamma}$  and  ${}_\xi R_{\mu'}^{m_1^\gamma m_2^\gamma}$ . The column of  $\beta G$  corresponds to the column of  ${}_\gamma R$  and  ${}_\xi R$  as  $m_1^\gamma$  and  $m_2^\gamma$  correspond to  $\alpha_1$  and  $\alpha_2$  through the dipole-selection rule.

$\Lambda^+$	$l$	$\beta G_{\Lambda^+}^{ll,\alpha_1\alpha_2}$						
		$\alpha_1\alpha_2$	$\sigma\sigma$	$\pi\sigma$	$\pi\pi$	$\delta\sigma$	$\delta\pi$	$\delta\delta$
II	1		-0.400	-1.200	-0.400			
	2		-0.286	-0.495	0.286	1.400	1.212	0.286
	3		-0.267	-0.327	0.400	1.461	0.894	0.0
	4		-0.260	-0.246	0.442	1.478	0.701	-0.104
	5		-0.256	-0.199	0.462	1.486	0.576	-0.154
			$\pi\pi$	$\delta\pi$	$\delta\delta$	$\phi\pi$	$\phi\delta$	$\phi\phi$
$\Delta$	1		0.200					
	2		-0.143	-1.212	-0.571			
	3		-0.200	-0.894	0.0	1.033	1.155	0.333
	4		-0.221	-0.701	0.208	1.237	1.031	0.091
	5		-0.231	-0.576	0.308	1.329	0.888	-0.026

$\Lambda^+$	$\mu'^a$	${}_\gamma R_{\mu'}^{m_1^\gamma m_2^\gamma}$						
		$m_1^\gamma m_2^\gamma$	$m_1^\gamma m_2^\gamma$	$m_1^\gamma m_2^\gamma$	$m_1^\gamma m_2^\gamma$	$m_1^\gamma m_2^\gamma$	$m_1^\gamma m_2^\gamma$	$m_1^\gamma m_2^\gamma$
$\Lambda^+$	$\mu'^a$	-1 -1	0 -1	0 0	1 -1	1 0	1 1	
$\Pi_{-1/2}$	-1/2	1.0	0.5	0.0	0.0	-0.5	-1.0	
$\Delta_{-3/2}$								

$\Lambda^+$	$\mu'^a$	${}_\xi R_{\mu'}^{m_1^\gamma m_2^\gamma}$						
		$m_1^\gamma m_2^\gamma$	$m_1^\gamma m_2^\gamma$	$m_1^\gamma m_2^\gamma$	$m_1^\gamma m_2^\gamma$	$m_1^\gamma m_2^\gamma$	$m_1^\gamma m_2^\gamma$	$m_1^\gamma m_2^\gamma$
$\Lambda^+$	$\mu'^a$	-1 -1	0 -1	0 0	1 -1	1 0	1 1	
$\Pi_{-1/2}$	-1/2	0.0	-0.125	0.0	-0.25	-0.125	0.0	
$\Delta_{-3/2}$								

<sup>a</sup>For transitions in Hund's case (a) and assuming that the initial state is a  ${}^1\Sigma^+$  ( $\Lambda''=0$  and  $\Sigma''=0$ ) we have  $\mu' = -\Sigma^+$  and  $\Sigma^+ = \frac{1}{2}$  giving  $\Omega^+ = -\frac{1}{2}$  and  $\Omega^+ = -\frac{3}{2}$  for the ionic states of symmetry  $\Pi^-$  and  $\Delta^-$ .

Similar relations can be derived for more general ionic spin states,

$$\begin{aligned} \beta_{\Lambda^+\Omega^+} &= \beta_{\Lambda^+\Omega^{+'}}, & \bar{P}_{\Lambda^+\Omega^+} &= -\bar{P}_{\Lambda^+\Omega^{+'}}, \\ \gamma_{\Lambda^+\Omega^+} &= -\gamma_{\Lambda^+\Omega^{+'}}, & \xi_{\Lambda^+\Omega^+} &= -\xi_{\Lambda^+\Omega^{+'}}, \end{aligned} \quad (20)$$

where  $\Omega^+$  and  $\Omega^{+'}$  are the sum of projections of the angular and the spin momenta onto the internuclear axis with  $\Lambda^{+'} = \Lambda^+$  and  $\Sigma^{+'} = -\Sigma^+$  ( $\Sigma^+$  not to be confused with the label of the molecular state  $\Sigma^+$ ). Particularly in the case of a triplet ionic state it can be demonstrated that in this approximation the contribution to the polarization parameters from the state with  $\Sigma^+ = 0$  projection of the spin is zero.

### B. Discussion of the generalized partitioning scheme and of some particular cases

A simple way to apply the partitioning scheme devised above is to develop numerical tables for the geometrical factors of each polarization parameter of the same type as the one introduced by Thiel<sup>17</sup> for the  $\beta$  asymmetry parameter. These tables give a rough estimate of any polarization parameter if the mixing between  $l$ 's is not too strong. This is done in the present section for Hund's case (a) and related to Hund's case (c) in Sec. II C. Of course, the qualitative estimates can be compared with a complete calculation taking into account all terms of the partitioning scheme.

In Tables III and IV we give the numerical values for  $\Pi$  and  $\Delta$  ionic cores of the diagonal and off-diagonal geometrical factors  $\beta G_{\Lambda^+}^{l_1 l_2, \alpha_1 \alpha_2}$  [Eq. (14)] and of the multiplicative factors  $\gamma R$  and  $\xi R$  defined below. Concerning  $\beta G$ , Tables III and IV are an extension of the table of Thiel<sup>17</sup> for  $\beta$  to a  $\Delta$  ionic core. The ratios  $\gamma R$  and  $\xi R$  are defined using Eqs. (14) as

$$\gamma R_{\mu'}^{m_1^\gamma, m_2^\gamma} = \gamma G_{\Lambda^+ \mu'}^{l_1 l_2, \alpha_1 \alpha_2} / \beta G_{\Lambda^+}^{l_1 l_2, \alpha_1 \alpha_2}, \quad (21a)$$

$$\xi R_{\mu'}^{m_1^\gamma, m_2^\gamma} = \xi G_{\Lambda^+ \mu'}^{l_1 l_2, \alpha_1 \alpha_2} / \beta G_{\Lambda^+}^{l_1 l_2, \alpha_1 \alpha_2}. \quad (21b)$$

The ratios  $\gamma R$  and  $\xi R$  are only functions of  $m^\gamma$  and  $\mu'$  as can be checked from (14). The relations between indices  $m^\gamma, \mu'$  and  $\alpha, \Omega^+$  (where  $\Omega^+ = \Lambda^+ + \Sigma^+$ ) are given by the dipole selection rule for the Hund's case (a) for the angular and spin momenta, namely,  $\Lambda'' + m^\gamma = \Lambda^+ + \lambda$  with  $\alpha = |\lambda|$  and  $\Sigma^{\Lambda''} = \Sigma^+ + \mu'$ . In the case of Tables III and IV we suppose that the initial state is totally symmetric and a singlet, i.e.,  $\Sigma^{\Lambda''} = 0$  which means  $\mu' = -\Sigma^+$ . Taking  $\mu' = -\frac{1}{2}$ , i.e.,  $\Sigma^+ = \frac{1}{2}$ , we obtain  $\Omega^+ = -\frac{1}{2}$  or  $\Omega^+ = -\frac{3}{2}$ , for  $\Pi$  and  $\Delta$  states with negative angular momentum projection. The  $\gamma R$  and  $\xi R$  coefficients of Tables III and IV can be calculated for other initial and final states. Strictly speaking  $\gamma R$  and  $\xi R$  should appear in a separate table. However, for ease of calculation of the geometrical factors of  $\gamma$  and  $\xi$ , we have kept them in the bottom of Tables III and IV.

Using (14) and (21) let us now calculate these ratios in particular cases. For simplicity, we use the absolute value for  $\gamma R$  and  $\xi R$ . The dipole selection rule restricts  $m^\gamma$  to the values 0,  $\pm 1$  and the difference  $m_2^\gamma - m_1^\gamma$  to the values 0,  $\pm 1$ ,  $\pm 2$ . Calculating explicitly the ratios

we have

$$\begin{aligned} |\xi R_{\mu'}^{\pm 1, \pm 1}| &= |\xi R_{\mu'}^{0, 0}| = 0 \quad (\text{selection rule}), \\ |\xi R_{\mu'}^{\pm 1, 0}| &= |\xi R_{\mu'}^{0, \pm 1}| = \frac{1}{8}, \\ |\xi R_{\mu'}^{\pm 1, \mp 1}| &= |\xi R_{\mu'}^{\mp 1, \pm 1}| = \frac{1}{4}, \end{aligned} \quad (22a)$$

and

$$\begin{aligned} |\gamma R_{\mu'}^{0, 0}| &= |\gamma R_{\mu'}^{\pm 1, \mp 1}| = 0 \quad (\text{selection rule}), \\ |\gamma R_{\mu'}^{\pm 1, \pm 1}| &= 1, \\ |\gamma R_{\mu'}^{\pm 1, 0}| &= |\gamma R_{\mu'}^{0, \pm 1}| = \frac{1}{2}. \end{aligned} \quad (22b)$$

In the case of  $\beta$  and  $\gamma$  we have the same dynamical factor containing a cosine of a phase difference and a geometrical factor which can be obtained from Tables III and IV. We can compare further  $\beta$  and  $\gamma$  for a  ${}^2\Pi_{3/2}$  ionic core if we write the following molecular partition:

$$\gamma_{\Pi_{3/2}} = \beta^{\sigma\sigma} + 0.5\beta^{\pi\sigma} - 0.5\beta^{\delta\pi} - \beta^{\delta\delta}, \quad (23a)$$

$$\beta_{\Pi_{3/2}} = \beta^{\sigma\sigma} + \beta^{\pi\sigma} + \beta^{\pi\pi} + \beta^{\delta\sigma} + \beta^{\delta\pi} + \beta^{\delta\delta}. \quad (23b)$$

In (23a) we have written directly  $\gamma$  in terms of  $\beta$  components and have omitted the ionic core label in the right-hand side of the equation. A linear combination  $a\beta + b\gamma$  eliminates the contribution from a particular term in (23). Such linear combinations can be used to analyze directly experimental results in terms of molecular channels.

Now we turn to the use of Tables III and IV as a qualitative tool to obtain a rough estimate of spin-polarization parameters. The procedure is the same as the one used by Thiel for  $\beta$ . First we estimate the leading transition moments and divide them by the cross section as in Eq. (10). Eventually in order to study the energy variation we calculate the trigonometric function of the Coulomb phase difference using Eq. (12'). Then we multiply these dynamical quantities with the geometrical factors and the ratio factor to get an approximate value of a parameter. If we restrict the summations to only one transition moment, the geometrical factor obtained from these tables will give the contribution to the spin-polarization parameter since the dynamical factor is 1.

Finally, let us discuss an example of a  ${}^2\Pi_{3/2}$  ionic core, the same as the one discussed by Cherepkov<sup>4</sup> and Heinzmann *et al.*<sup>2</sup> The expressions of  $\xi$  and  $\gamma$  for a  ${}^2\Pi_{3/2}$  ionic core can be separated into an atomiclike and a molecularlike contribution. Using the notations of Eqs. (7)–(9) and neglecting the subscript  $\Lambda^+\Omega^+$  in the right-hand side of the equation, we have for  $\xi$

$$\begin{aligned} \xi_{\Pi_{3/2}}^{\text{at}} &= \frac{1}{4}\sqrt{3/5}[M^{ds, \pi\sigma} \sin(\Phi^{ds, \pi\sigma}) \\ &+ 2\sqrt{2}M^{ds, \delta\sigma} \sin(\Phi^{ds, \delta\sigma})]. \end{aligned} \quad (24a)$$

From (24a) and (18a) it is obvious that  $\xi^{\text{at}} = \xi^{ds}$  showing that if atomiclike character is expected,  $\xi^{ds}$  will be the leading term in the partitioning scheme. If in  $\Phi^{ds, \pi\sigma}$  and  $\Phi^{ds, \delta\sigma}$  we neglect the molecular-type eigenphases, these eigenphases become atomiclike and we recover the Heinzmann *et al.*<sup>2</sup> equation (11) with inverted sign,

TABLE IV. Off-diagonal terms  $\beta G_{\Lambda^+}^{l+2, \alpha_1 \alpha_2}$  and the ratios  ${}_y R$  and  ${}_z R$ . The column of  $\beta G$  corresponds to the column of  ${}_y R$  and  ${}_z R$  as  $m_1^y$  and  $m_2^y$  correspond to  $\alpha_1$  and  $\alpha_2$  through the dipole-selection rule.

$\Lambda^+$ $\Pi$	$l^a$	$\alpha_1 \alpha_2$		$\beta G_{\Lambda^+}^{l+2, \alpha_1 \alpha_2}$					
		$\sigma\sigma$	$\pi\sigma$	$\pi\pi$	$\delta\sigma$	$\delta\pi$	$\delta\delta$		
		$l_\pi = l + 2; l_\sigma = l$	$l_\pi = l; l_\sigma = l + 2$	$l_\sigma = l + 2; l_\pi = l$	$l_\sigma = l; l_\pi = l + 2$	$l_\delta = l + 2; l_\pi = l$	$l_\delta = l; l_\pi = l + 2$	$l_\delta = l + 2; l_\pi = l$	$l_\delta = l; l_\pi = l + 2$
	0	0.894	1.549		2.191				
	1	0.786	1.283	-1.283	1.434	-1.434			
	2	0.767	1.212	-1.400	1.212	0.313	-1.400	0.495	0.495
	3	0.760	1.177	-1.441	1.101	0.416	-1.348	0.645	0.603
$\Delta$	$l$	$\pi\pi$	$\delta\pi$	$\delta\delta$	$\phi\pi$	$\phi\delta$	$\phi\phi$		
		$l_\delta = l + 2; l_\pi = l$	$l_\delta = l; l_\pi = l + 2$	$l_\delta = l + 2; l_\pi = l$	$l_\delta = l; l_\pi = l + 2$	$l_\phi = l + 2; l_\delta = l$	$l_\phi = l; l_\delta = l + 2$		
	1	0.641	1.434	-0.990	2.484	-1.309			
	2	0.700	1.400	-0.990	1.852	-1.309			
	3	0.721	1.348	-1.206	1.557	0.186	-1.393	0.350	0.402
		$m_1^y m_2^y$	$m_1^y m_2^y$	$m_1^y m_2^y$	$m_1^y m_2^y$	$m_1^y m_2^y$	$m_1^y m_2^y$	$m_1^y m_2^y$	$m_1^y m_2^y$
		$\mu'^b$	$\mu'^b$						
	$\Lambda^+$	-1 -1	0 -1	0 0	-1 1	0 1	1 0	1 1	1 1
	$\Pi_{-1/2}$	1.0	0.5	0.0	0.0	-0.5	-0.5	-1.0	
	$\Delta_{-3/2}$								
		$m_1^y m_2^y$	$m_1^y m_2^y$	$m_1^y m_2^y$	$m_1^y m_2^y$	$m_1^y m_2^y$	$m_1^y m_2^y$	$m_1^y m_2^y$	$m_1^y m_2^y$
	$\Lambda^+$	-1 -1	0 -1	0 0	-1 1	0 1	1 0	1 1	1 1
	$\Pi_{-1/2}$	0.0	-0.125	0.0	-0.25	-0.125	-0.125	0.0	
	$\Delta_{-3/2}$								
		$m_1^y m_2^y$	$m_1^y m_2^y$	$m_1^y m_2^y$	$m_1^y m_2^y$	$m_1^y m_2^y$	$m_1^y m_2^y$	$m_1^y m_2^y$	$m_1^y m_2^y$

<sup>a</sup>The listed terms are  $\beta G_{\Lambda^+}^{l+2, \alpha_1 \alpha_2}$  or  $\beta G_{\Lambda^+}^{l+2, \alpha_1 \alpha_2}$  depending on the columns of the table.  
<sup>b</sup>For transitions in Hund's case (a) and assuming that the initial state is a  ${}^1\Sigma^+$  ( $\Lambda''=0$  and  $\Sigma''=0$ ) we have  $\mu' = -\Sigma^+$  and  $\Sigma^+ = \frac{1}{2}$  giving  $\Omega^+ = -\frac{1}{2}$  and  $\Omega^+ = -\frac{1}{2}$  for the ionic states of symmetry  $\Pi^-$  and  $\Delta^-$ .



$$\xi_{\Pi_{3/2}}^{\text{mol}} = \frac{1}{2} \left[ \begin{aligned} & \frac{2}{7} \sqrt{6} M^{dd, \delta\sigma} \sin(\Phi^{dd, \delta\sigma}) \\ & - \frac{\sqrt{3}}{14} M^{dd, \pi\sigma} \sin(\Phi^{dd, \pi\sigma}) \\ & + \frac{3}{7\sqrt{2}} M^{dd, \delta\pi} \sin(\Phi^{dd, \delta\pi}) \\ & - \frac{3}{10} M^{pp, \pi\sigma} \sin(\Phi^{pp, \pi\sigma}) \end{aligned} \right]. \quad (24b)$$

The molecular contribution has two components  $\xi^{dd}$  and  $\xi^{pp}$  and it is reduced to zero if we disregard the molecular eigenphase due to the phase difference between functions of same  $l$  but different  $\lambda$ .

In the case of  $\gamma$  the atomic-molecular partitioning is more difficult as we have atomic and molecular contributions to the same  $l_1 l_2$  term. Let us start by writing the exact formula for  $\gamma$  for a  ${}^2\Pi_{3/2}$  core neglecting in the right-hand part of (25) the ionic core index as above

$$\gamma_{\Pi_{3/2}} = \gamma^{dd} + \gamma^{ds} + \gamma^{pp}, \quad (25a)$$

with the notations

$$\gamma^{dd} = \frac{2}{7} (M^{dd, \sigma\sigma} + M^{dd, \delta\delta}) + \frac{\sqrt{3}}{7} M^{dd, \pi\sigma} \cos(\Phi^{dd, \pi\sigma}) + \frac{3\sqrt{2}}{7} M^{dd, \delta\pi} \cos(\Phi^{dd, \delta\pi}), \quad (25b)$$

$$\gamma^{ds} = - \left[ \begin{aligned} & \frac{2}{\sqrt{5}} M^{ds, \sigma\sigma} \cos(\Phi^{ds, \sigma\sigma}) \\ & - \sqrt{3/5} M^{ds, \pi\sigma} \cos(\Phi^{ds, \pi\sigma}) \end{aligned} \right], \quad (25c)$$

$$\gamma^{pp} = \frac{2}{5} M^{pp, \sigma\sigma} + \frac{3}{5} M^{pp, \pi\sigma} \cos(\Phi^{pp, \pi\sigma}). \quad (25d)$$

As the initial orbital is  $p$ , using the atomic selection rules we find that in (25)  $\gamma^{dd}$  and  $\gamma^{ds}$  contain atomic and molecular contributions whereas  $\gamma^{pp}$  contains only molecular ones. A further simplification of (25) occurs if we neglect the molecular eigenphases [see Eqs. (12) and (12')],

$$\Phi^{dd, \pi\sigma} = 0, \quad (26a)$$

$$\Phi^{ds, \sigma\sigma} = \Phi^{ds, \pi\sigma} = \eta_d - \eta_s, \quad (26b)$$

$$\Phi^{pp, \pi\sigma} = 0. \quad (26c)$$

From (26) we see that by neglecting the molecular eigenphases we do not reduce the number of terms in (25) but rather maximize  $\gamma^{dd}$  and  $\gamma^{pp}$  and change the value of the cross term  $\gamma^{ds}$ . This cross term is the only one which is dependent on the difference of the Coulomb phase and therefore has a rapid variation with the energy near the threshold.

We have completed our analysis of a  $p$  excitation giving the  $\Pi_{3/2}$  ionic state. Another example, namely excitation from a  $d$  shell, will be discussed in Sec. III C.

### C. Extension of the formalism to Hund's coupling case (c)

The formulas of Cherepkov have been deduced in Hund's coupling cases (a) or (b) for both the initial, the final, and the ionic states, i.e., in the case where the quantum numbers  $\Lambda$ ,  $S$ , and  $\Sigma$  (projection of the spin angular momentum  $S$  on the internuclear axis) are well defined in the absence of rotation. In the following, we continue to describe the initial state in Hund's case (b) because the initial state is assumed to be here the ground state of the neutral molecule, namely,  ${}^1\Sigma^+$  for the molecules studied in this paper. In Secs. II A and II B the spin-polarization parameters have been defined for specified values of the quantum numbers  $\Lambda^+$  and  $\Omega^+ = \Lambda^+ + \Sigma^+$  of the substates of the ion. Note that in fact each spectroscopic substate  $|\Omega^+|$  is doubly degenerate (for a nonrotating molecule) with two components corresponding to the signed values  $\Omega^+$  and  $-\Omega^+$ . In his papers, Cherepkov has characterized the ion state by  $\Lambda^+$ ,  $S^+$ , and  $M_S$  which is denoted here  $\Sigma^+$ .

To obtain a final ionic state with a given value of  $\Omega^+$ , the total final state must be described by the  $(\Omega_c, \omega)$  coupling (see Ref. 28, p. 338) and characterized by the value of  $\Omega = \Omega_c + \omega = \Omega^+ + \omega$ , where  $\omega = \lambda + \mu'$ . The case of a  $(\pi)^3$  ionic state is discussed in Ref. 5. For example, from Fig. 1 of Ref. 5 we see that the final states of the configuration  $(\pi)^3 (\epsilon\sigma)$ , which are ionized in the  ${}^2\Pi_{3/2}$  substate have two possible values of  $\Omega$ :  $\Omega = 1$  and 2. If the initial state is  $0^+ ({}^1\Sigma_0^+)$ , the final states of the dipole-allowed transition have only  $\Omega = 1$ . In the case where the influence of rotation is neglected,  $\Lambda$  also remains a good quantum number and the wave functions converging to a core with a definite  $\Omega^+$  value are given by<sup>5</sup>

$$\frac{1}{\sqrt{2}} [\psi({}^1\Lambda_\Omega) \pm \psi({}^3\Lambda_\Omega)]. \quad (27)$$

It is easy to see that, because the intensity comes only from the  ${}^1\Lambda_\Omega$  state, the formalism of Cherepkov, established for a final state with  $\Lambda$  and  $S$  specified, remains valid for a state with the value of  $\Omega$  specified.

In the general case of an ionization of a  $l''$  shell, if the electronic energy splitting,  $\Delta E$ , between the molecular electronic ion states, corresponding to nondegenerate  $\Lambda^+$  different values, is large relative to the spin-orbit splitting ( $\Lambda^+ A$ ), the Hund's coupling case (a) is well adapted. If  $\Omega^{+'} = \Omega^+ + 1$ , we obtain from (20)

$$\sigma_{\Lambda^+ \Omega^+} = \sigma_{\Lambda^+ \Omega^+ + 1}, \quad (28a)$$

$$\beta_{\Lambda^+ \Omega^+} = \beta_{\Lambda^+ \Omega^+ + 1},$$

and the relations between the spin-polarization parameters are that given by Cherepkov<sup>4,24</sup> and Eq. (20),

$$\xi_{\Lambda^+ \Omega^+} = -\xi_{\Lambda^+ \Omega^+ + 1}, \quad (28b)$$

$$\xi_{\Lambda^+ = 0, \Omega^+} \equiv 0,$$

and similar relations for the other spin-polarization parameters. The corresponding partial cross section leading to the ion in the  $\Lambda^+$  state is

TABLE V. Projection of the  $(J, M_J)$  atomic wave functions in the  $J_a^+ \Omega^+$  Hund's case (c) molecular wave functions expressed as combinations of Hund's case (a) wave functions ( $p$  configuration).

	$J$	$M_J$	Atomic functions	$J_a^+$	$\Omega^+$	Molecular functions
${}^2P_{3/2}$	$\frac{3}{2}$	$\frac{3}{2}$	$ p_{+1} $	$\frac{3}{2}$	$\frac{3}{2}$	${}^2\Pi_{3/2}$
	$\frac{3}{2}$	$\frac{1}{2}$	$\frac{1}{\sqrt{3}}(\sqrt{2} p_0  +  \overline{p_{+1}} )$	$\frac{3}{2}$	$\frac{1}{2}$	$\frac{1}{\sqrt{3}}(\sqrt{2}{}^2\Sigma_{1/2}^+ + {}^2\Pi_{1/2})$
${}^2P_{1/2}$	$\frac{1}{2}$	$\frac{1}{2}$	$\frac{1}{\sqrt{3}}( p_0  - \sqrt{2} \overline{p_{+1}} )$	$\frac{1}{2}$	$\frac{1}{2}$	$\frac{1}{\sqrt{3}}({}^2\Sigma_{1/2}^+ - \sqrt{2}{}^2\Pi_{1/2})$

$$\sigma_{\Lambda^+} = \sum_{\Omega^+} \sigma_{\Lambda^+ \Omega^+}, \quad (28c)$$

$$\beta_{\Lambda^+} = \beta_{\Lambda^+ \Omega^+} = \beta_{\Lambda^+ \Omega^+ + 1}.$$

If now, the electronic energy is small compared to the spin-orbit energy, the ionic state is better described in terms of Hund's coupling case (c). The correlation diagram of Fig. 2 shows, in the case of  $p$  ionization, that in the limit case (c), the good quantum numbers for the ion states are  $(J_a^+, \Omega^+)$  where  $J_a^+ = L^+ + S^+$  with  $L^+$  well approximated by the  $l$  atomic value.<sup>29</sup> These states  $(J_a^+, \Omega^+)$  are correlated to the  $(J, M_J)$  atomic states and the resulting case (c) ion functions can be expressed as linear combinations of case (a) wave functions, with the coefficients  $C_{\Lambda^+ \Omega^+}^{J_a^+}$ . An example is given in Table V for  $p$  ionization. The cross sections calculated for the Hund's case (c) are expressed in terms of the cross sections for the Hund's case (a) of the ion, namely,

$$\sigma_{J_a^+} = \sum_{\Omega^+, \Lambda^+} (C_{\Lambda^+ \Omega^+}^{J_a^+})^2 \sigma_{\Lambda^+ \Omega^+},$$

and similarly for the angular distribution asymmetry parameters

$$\beta_{J_a^+} = \frac{\sum_{\Omega^+, \Lambda^+} (C_{\Lambda^+ \Omega^+}^{J_a^+})^2 \beta_{\Lambda^+ \Omega^+} \sigma_{\Lambda^+ \Omega^+}}{\sum_{J_a^+} \sigma_{J_a^+}}. \quad (29a)$$

We have similar relations for spin-polarization parameters. Thus the relations in the case of ionization of a  $l''$  shell are

$$\sigma_{J_a^+} = \frac{l''}{l''+1} \sigma_{J_a^+ + 1},$$

$$\beta_{J_a^+} = \beta_{J_a^+ + 1}, \quad (29b)$$

$$\xi_{J_a^+} = -\frac{l''+1}{l''} \xi_{J_a^+ + 1},$$

and similar relations for other spin-polarization parameters. They are similar to the relations obtained in the atomic case.

The total cross section corresponding to a  $l''$  hole is given by

$$\sigma^{l''} = \sum_{\Lambda^+} \sigma_{\Lambda^+} = \sum_{J_a^+} \sigma_{J_a^+}$$

and the corresponding averaged  $\beta^{l''}$  is

$$\beta^{l''} = \frac{\sum_{\Lambda^+} \sigma_{\Lambda^+} \beta_{\Lambda^+}}{\sum_{\Lambda^+} \sigma_{\Lambda^+}} = \frac{\sum_{J_a^+} \sigma_{J_a^+} \beta_{J_a^+}}{\sum_{J_a^+} \sigma_{J_a^+}} \quad (30a)$$

and following (29b)

$$\beta^{l''} = \beta_{J_a^+} = \beta_{J_a^+ + 1}. \quad (30b)$$

The intermediate case between coupling case (a) and (c), presented in Fig. 2, will be explained in the particular case of a  $p$  ionization in Sec. III B. All these formulas are valid in the approximation of the nonrelativistic continuum wave functions used through this paper.

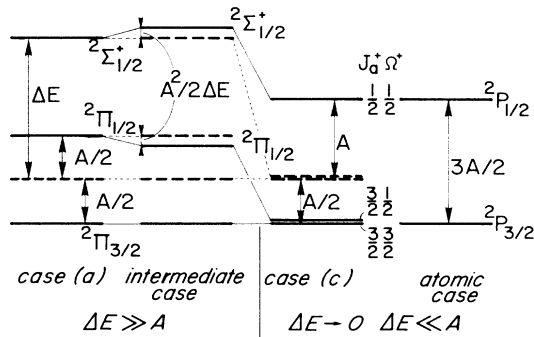


FIG. 2. Correlation diagram between Hund's case (a) and case (c) in the case of  $(\pi np)^3$  and  $\sigma np$  configurations for the ion states. In pure case (a), the off-diagonal spin-orbit interaction between the  ${}^2\Pi_{1/2}$  and  ${}^2\Sigma_{1/2}^+$  ion substates equal to  $A/\sqrt{2}$  is neglected. It is taken into account by second-order perturbation theory for the case intermediate between case (a) and case (c). Finally, the pure case (c) is obtained by diagonalizing the  $2 \times 2$  spin-orbit matrix between the  ${}^2\Pi_{1/2}$  and  ${}^2\Sigma_{1/2}^+$  substates, electronically degenerate.

### III. RESULTS AND DISCUSSION

We have studied the  $\pi np$  outer-shell and  $(n-1)d$  inner-shell photoionization of two hydrogen halides, HBr and HI. Except for the  $\pi 4p$  ionization of HBr, the total cross sections have been published previously<sup>30,31</sup> and we will discuss here mainly the photoelectron spin-polarization parameters.

### A. Framework of the *ab initio* calculations

The continuum wave functions have been obtained in the frozen-core static-exchange approximation, using the method previously developed<sup>32,33</sup> for light molecules, and as already reported<sup>5</sup> extended to  $\delta$  and  $\phi$  symmetries. The transition moments have been calculated in the dipole length approximation and the molecular orbitals of the ground state of the neutral molecule calculated for the equilibrium internuclear distance have been used to describe the orbitals of the ion core.

The calculations have been performed at the Centre Inter Regional de Calcul Electronique (CIRCE) Computer Center of the CNRS.

The configuration of the  $X^1\Sigma^+$  ground state of the two molecules studied is

$$C(\sigma ns)^2(\sigma np)^2(\pi np)^4(\sigma nd)^2(\pi nd)^4(\delta nd)^4 \\ [\sigma(n+1)s]^2[\sigma(n+1)p]^2[\pi(n+1)p]^4,$$

where  $C$  designates the  $KL$  core shells for HBr and the  $KLM$  core shells for HI. The quantum number  $n$ , which holds for the main constituent orbital of the halogen atom of a given molecular orbital, is 3 for HBr and 4 for HI.

The ionization of the  $\pi(n+1)p$  orbital gives a resulting  $X^2\Pi$  ion which is split by the spin-orbit interaction into two substates  $^2\Pi_{1/2}$  and  $^2\Pi_{3/2}$ , whereas the ionization of an  $nd$  orbital gives rise to three possible ion states  $(\sigma nd)^{-1}2\Sigma^+$ ,  $(\pi nd)^{-1}2\Pi$ , and  $(\delta nd)^{-1}2\Delta$ . The spin-orbit contribution for the  $2\Sigma^+$  state is zero. The  $2\Pi$  state is split into  $^2\Pi_{1/2}$  and  $^2\Pi_{3/2}$  substates and the  $2\Delta$  into  $^2\Delta_{3/2}$  and  $^2\Delta_{5/2}$  substates. The final states which have a nonzero transition moment from the ground state have the  $1\Sigma^+$  and  $1\Pi$  symmetries, namely, for the  $\pi p$  ionization,

$$\begin{aligned} &(^2\Pi, \epsilon\pi)^1\Sigma^+, \\ &(^2\Pi, \epsilon\sigma)^1\Pi, \\ &(^2\Pi, \epsilon\delta)^1\Pi, \end{aligned}$$

i.e., three continuum states, and for the  $d$  ionization

$$\begin{array}{lll} (^2\Sigma^+, \epsilon\sigma)^1\Sigma^+ & (^2\Pi, \epsilon\pi)^1\Sigma^+ & (^2\Delta, \epsilon\delta)^1\Sigma^+ \\ (^2\Sigma^+, \epsilon\pi)^1\Pi & (^2\Pi, \epsilon\sigma)^1\Pi & (^2\Delta, \epsilon\pi)^1\Pi \\ & (^2\Pi, \epsilon\delta)^1\Pi & (^2\Delta, \epsilon\phi)^1\Pi \end{array}$$

i.e., eight continuum states.

To see whether Hund's case (a) or case (c) representation is better adapted to the ion state, it is necessary to compare the electronic energy difference with the spin-orbit splitting. For  $np$  ionization, two molecular states are obtained: the  $X^2\Pi$  ionic ground state which corresponds to the  $\pi np$  ionization and the  $A^2\Sigma^+$  excited state which corresponds to the  $\sigma np$  ionization. The energy difference between the  $^2\Pi_{1/2}$  and  $^2\Sigma^+$  states is 3.2 and 2.8 eV for HBr and HI, respectively.<sup>34</sup> This is large compared to the spin-orbit splitting,  $A$ , between the two sublevels  $X^2\Pi_{3/2}$  and  $X^2\Pi_{1/2}$  which is 0.33 and 0.66 eV for HBr and HI, respectively.<sup>34</sup> Consequently, for the  $\pi np$  ionization, the  $X^2\Pi$  ionic state is well represented

in Hund's case (a). This point will be discussed further in Sec. III B.

In the case of  $d$  inner-shell ionizations, the electronic splitting of the three ionic molecular states  $2\Sigma^+$ ,  $2\Pi$ , and  $2\Delta$  is not known experimentally. By calculation, we have obtained<sup>31</sup> energy intervals of 0.38 and 0.47 eV for HBr and HI, respectively. This is smaller than the spin-orbit splittings of the Br atom and the I atom in their  $2D$  state which are 1.05 (Ref. 35) and 1.9 eV (Ref. 36), respectively. Consequently, the Hund's case (c) representation must be used to describe the  $d$  hole. The expressions of these functions in terms of the Hund's case (a) have been given elsewhere.<sup>37</sup> If the electronic splitting of the ionic  $2\Sigma^+$ ,  $2\Pi$ , and  $2\Delta$  states is taken equal to zero, we obtain two states with  $J_a^+ = 3/2$  and  $5/2$  which are related to the  $^2D_{3/2}$  and  $^2D_{5/2}$  ionic atomic states. This description is in agreement with the observation of only two peaks in the photoelectron spectrum with a splitting of 1.05 eV for HBr (Ref. 38) and 1.76 eV for HI,<sup>39</sup> in each case very similar to the spin-orbit splitting of the states of the corresponding atoms.

### B. $\pi np$ outer-shell ionization in HBr and HI

For  $\pi np$  ionization, the experimental cross sections present a Cooper minimum. The calculated cross section for HBr is presented in Fig. 3. At low energies it compares better with the experimental results of Carlson *et al.*<sup>40</sup> than with those of Brion *et al.*<sup>41</sup> However, in this static exchange calculation, the Cooper minimum appears only in the  $\sigma_{\Pi}^{\delta}$  and  $\sigma_{\Pi}^{\pi}$  contributions, not in the

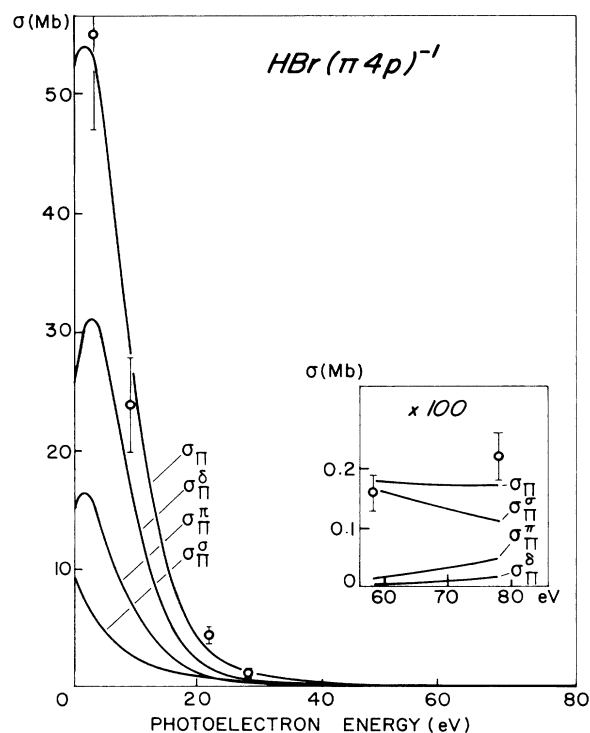


FIG. 3. Partial photoionization cross section of HBr ( $\pi 4p^{-1}$ ) showing the contributions of the  $\sigma$ ,  $\delta$ , and  $\pi$  waves. The experimental points are taken from Ref. 40.

total  $\sigma_{\Pi}$  cross section since the contribution from  $\sigma_{\Pi}^{\sigma}$  is dominant in this energy region. Figures 4(a) and 4(b) give the variation with energy of the  $\beta$  angular distribution and  $\bar{P}$ ,  $\gamma$ ,  $\xi$  spin-polarization parameters for HBr ( $\pi 4p$ )<sup>-1</sup> and HI ( $\pi 5p$ )<sup>-1</sup> ionizations. The calculation of the  $\beta$  parameter for HBr compares well with the experimental results of Carlson *et al.*<sup>40</sup> Those for HI have been previously reported<sup>30</sup> but are reproduced in Fig. 4(b) for comparison with HBr. The variation with energy of the spin-polarization parameters is comparable in HBr and HI and follows that obtained for the  $p$  ionization of the isoelectronic atoms,  $4p$ <sup>-1</sup> in krypton<sup>9</sup> and  $5p$ <sup>-1</sup> in xenon (Fig. 4 of Ref. 10). In particular, the values at the Cooper minimum are practically the same in the two molecules.

We start the discussion with the polarization parameter,  $\bar{P}$ , which depends only on the modulus of the transition moments. The formula (19b) for  $\bar{P}$  in terms of  $\sigma_{\Lambda^+}^{\lambda}$  [Eq. 19(a)] applied to a  $\Pi$  core is

$$\begin{aligned} \bar{P}_{\Pi_{1/2}} &= \frac{1}{2} \left[ \sum_{l=0}^{\infty} M_{\Pi_{1/2}}^{ll, \sigma\sigma} - \sum_{l=2}^{\infty} M_{\Pi_{1/2}}^{ll, \delta\delta} \right] \\ &= \frac{1}{2\sigma_{\Pi}} (\sigma_{\Pi_{1/2}}^{\sigma} - \sigma_{\Pi_{1/2}}^{\delta}). \end{aligned} \quad (31)$$

As pointed by Thiel,<sup>42</sup> the cross section at the Cooper minimum is dominated by the  $s\sigma$  wave and, consequently, in formula (31)  $\sigma_{\Pi_{1/2}}^{\delta}$  can be neglected relative to  $\sigma_{\Pi_{1/2}}^{\sigma}$  partial cross section.  $\bar{P}_{\Pi_{1/2}}$  reaches its maximum value of 0.5 which is half the maximum value of  $\bar{P}_{1/2}$  in the corresponding atom, because here Hund's case (a) is used for the molecule.

Partitioning analysis of Sec. II B can be used to single out the main contributions to  $\xi$  and  $\gamma$ . For  $\xi$ , the dominant term is the atomic term (Eq. 24a),  $\xi^{ds}$ , which follows the energy variation of the cross section. The molecular contribution,  $\xi^{dd}$ , is about ten times smaller than the atomic one. This term decreases at high energy

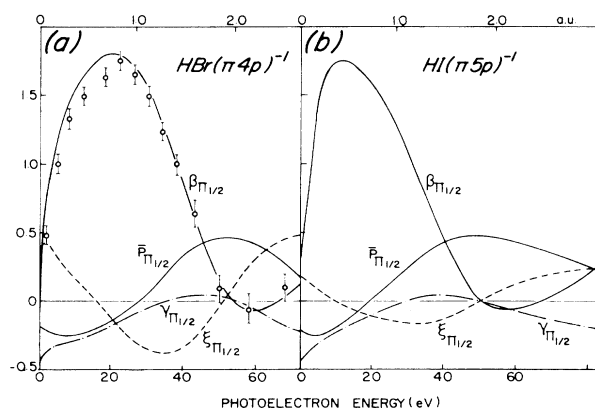


FIG. 4. (a) Angular asymmetry parameter  $\beta$  and spin polarization parameters  $\bar{P}$ ,  $\gamma$ , and  $\xi$  as function of energy for  $X^2\Pi_{1/2}(\pi 4p)^{-1}$  of HBr. The parameters  $\beta$ ,  $\bar{P}$ ,  $\gamma$ , and  $\xi$  are dimensionless. The experimental points are taken from Ref. 40. (b) The same for HI ( $\pi 5p$ )<sup>-1</sup>.

since the electron becomes less sensitive to the molecular field when the energy increases. As said above, the transition moment due to  $l \neq 0$  is negligible at the Cooper minimum and consequently  $\xi \rightarrow 0$ .

For  $\gamma$ , the dominant term is  $\gamma^{dd}$  [Eq. (25b)]. Consequently,  $\gamma$  has no contribution from  $l=0$  at the Cooper minimum, and is zero.

The maximum in the cross section near the threshold (see Fig. 3) is dominated by the  $d$  continuum wave. Therefore, we can discuss this energy region in terms of atomic  $d$  contributions. The atomic transition moments corresponding to the  $\pi np \rightarrow \epsilon d\sigma$ ,  $\pi np \rightarrow \epsilon d\pi$ , and  $\pi np \rightarrow \epsilon d\delta$  are in the ratio  $1:\sqrt{3}:\sqrt{6}$ , respectively. If we suppose that these ratios are conserved in the molecule, and use them in Eq. (31), we have

$$\bar{P}_{\Pi_{1/2}} = -0.25 \quad (32)$$

for a pure  $p \rightarrow d$  transition. In these molecules, the first maxima of  $\bar{P}_{\Pi_{1/2}}$ , corresponding to the maximum in the total cross section, have exactly this value. This means that for  $\bar{P}$ , the molecular effects are negligible. The maximum values for the other parameters [Figs. 4(a) and 4(b)] are also very similar to  $\bar{P}_{1/2}$  of the corresponding atoms divided by two, as explained above. The explanation of the atomlike behavior of these parameters is that the  $\pi np$  molecular orbital is a nonbonding orbital.

We have compared the molecular quantities to the atomic parameters at low energy. At high energy, the static exchange or monoconfigurational approximation becomes less valid and it would be necessary to introduce the interchannel couplings due to the opening of new channels in order to compare with the atomic results which have been obtained with RPAE calculations. A more sophisticated calculation described elsewhere<sup>30</sup> has introduced the interchannel coupling between the  $\pi 5p$ <sup>-1</sup> and  $\pi 4d$ <sup>-1</sup> channels for HI at two values of the energy. In Table VI, we compare the numerical results obtained in these two different calculations. The interchannel coupling improves the  $\beta$  values compared to the experiment.<sup>43</sup> Unfortunately, the  $\gamma$  values seem inconsistent with the RPAE calculations in atoms. This could be due to the fact that in our calculation only a restricted part of the electronic correlation has been introduced.

Now, we must consider here the validity of Hund's case (a) for  $\pi p$  ionization. Experimentally, the  $A$  spin-orbit splitting of the  $^2\Pi$  state is equal to about  $\frac{2}{3}$  of the atomic  $^2P$  splitting, that is to say, that which is expected from a correlation diagram in Hund's case (a) (see Fig. 2 or, for example, Fig. 4.17, p. 235 of Ref. 29). This confirms the validity of the relations (28),

$$\xi_{\Pi_{3/2}} = -\xi_{\Pi_{1/2}} \quad (33)$$

and

$$\xi_{\Sigma_{1/2}^+} \equiv 0. \quad (34)$$

A departure from formula (33) can be due to the kinetic energy effect, that is to say, the relation (33) holds only for equal kinetic energy of the photoelectrons issued from different thresholds. This is why our values

TABLE VI. Comparison between values of HI parameters before and after interchannel coupling (IC) (Ref. 30).

$h\nu$ (eV)	71		92	
	Before IC	After IC $\pi 5p^{-1}$	Before IC	After IC
$\sigma$ (Mb)	0.19	0.24 (0.92) <sup>a</sup>	0.16	0.25 (0.79) <sup>a</sup>
$\beta_{\Pi}$	-0.05	0.96 (0.90) <sup>a</sup>	0.24	1.43 (1.60) <sup>a</sup>
$\bar{P}_{1/2}$	0.42	0.30	0.24	0.11
$\gamma_{1/2}$	-0.07	0.07	-0.17	0.11
$\xi_{1/2}$	0.14	0.19	0.25	0.18
	$\pi 4d^{-1}$			
$\sigma_{\Pi}$ (Mb)	9.16	9.08	10.66	10.52
$\beta_{\Pi}$	0.78	0.81	0.75	0.72
$\bar{P}_{\Pi 1/2}$	-0.09	-0.09	-0.13	-0.11
$\gamma_{\Pi 1/2}$	-0.23	-0.23	-0.20	-0.21
$\xi_{\Pi 1/2}$	0.04	0.03	0.05	0.04

<sup>a</sup>Experimental values from Ref. 43.

are reported as function of the photoelectron energy and not of the photon energy. However, such a kinetic energy effect cannot be invoked to explain the departure from Eq. (33) observed for the experimental  $\xi$  in  $\text{CH}_3\text{I}$  and  $\text{CH}_3\text{Br}$ .<sup>3</sup> This effect will give a modification in the opposite sense of the observed value. A departure from the relation (34) could be due to the fact that the actual representation corresponds to an intermediate case between the Hund's case (a) and case (c). More precisely, there exists a spin-orbit interaction  $H_{\text{SO}}$  between the  $X^2\Pi_{1/2}$  and  $A^2\Sigma_{1/2}^+$  states which, in the pure precession hypothesis, has the value

$$\langle \psi(A^2\Sigma_{1/2}^+) | H_{\text{SO}} | \psi(X^2\Pi_{1/2}) \rangle = A/\sqrt{2}. \quad (35)$$

Thus the wave functions intermediate between the Hund's case (a) and (c) can be obtained by the first-order perturbation theory

$$\begin{aligned} \Psi(^2\Pi_{1/2}) &= \psi(^2\Pi_{1/2}) - \frac{A}{\sqrt{2}\Delta E} \psi(^2\Sigma_{1/2}^+), \\ \Psi(^2\Sigma_{1/2}^+) &= \psi(^2\Sigma_{1/2}^+) + \frac{A}{\sqrt{2}\Delta E} \psi(^2\Pi_{1/2}), \end{aligned} \quad (36)$$

where  $\Delta E$  is the energy difference between the  $^2\Sigma_{1/2}^+$  and  $^2\Pi_{1/2}$  states (see Fig. 2). This gives, for example, for HI, corresponding to the  $\Psi$  wave function (36),  $\xi_{\Sigma_{1/2}^+} \approx 0.03\xi_{\Pi_{1/2}}$  for same photoelectron energy if  $\sigma_{\Sigma_{1/2}^+} = \sigma_{\Pi_{1/2}}$ . If the two  $^2\Pi_{1/2}$  and  $^2\Sigma_{1/2}^+$  states are electronically degenerate, Hund's case (c) wave functions must be used for the core. In Table V the transformation formulas which express the functions of case (c) in terms of functions of case (a) are given for the  $p$  configuration of the ion (in place of  $p^3$ ). These  $(J_a^+, \Omega^+)$  functions are correlated to the  $(J, M_J)$  atomic functions expressed as linear combinations of determinants built

on  $p_{ml}$  functions. The  $\beta$  spin is designated by a bar upon the function. Only the functions with positive values of  $M_J$  and  $\Omega^+$  are given. In this case, two  $(J_a^+, \Omega^+)$  molecular states, namely, the  $(3/2, 3/2)$  and  $(3/2, 1/2)$  states, become degenerate in energy and the splitting with the  $(1/2, 1/2)$  state becomes equal to the  $^2P_{3/2}, ^2P_{1/2}$  atomic splitting, i.e.,  $\frac{3}{2}A$  (see Fig. 2). Also the relations between the spin-polarization parameters become identical to that for the  $^2P$  ionic atoms, namely [cf. Eq. (29b), with  $l''=1$ ],

$$\xi_{1/2} = -2\xi_{3/2}. \quad (37)$$

Such an example could appear in the heterogeneous rare-gas dimer ions such as the  $\text{XeAr}^+$  molecule or in other heavy ions such as  $\text{HgKr}^+$ ,  $\text{HgXe}^+$ ,  $\text{TlBr}^+$ , or  $\text{InI}^+$ .

### C. $d$ inner-shell ionization

The total cross sections corresponding to  $d$  inner-shell ionization have been previously reported for  $3d^{-1}$  of HBr and  $4d^{-1}$  of HI.<sup>31</sup> They are identical in Hund's coupling case (a) or case (c) [see Eq. (30)]. The spin-

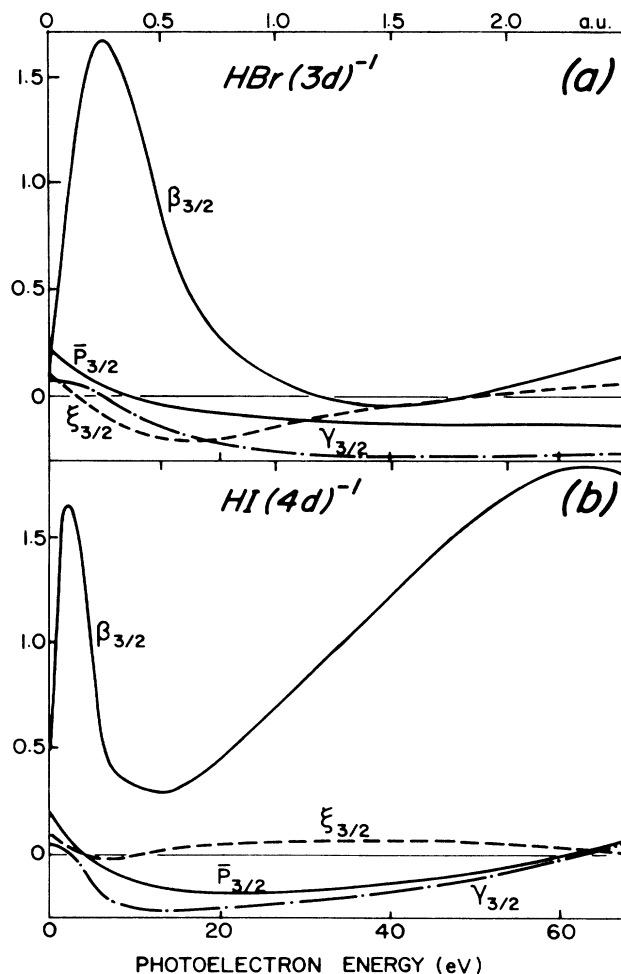


FIG. 5. (a) Same parameters as in Fig. 4 for HBr ( $3d^{-1}$ ). (b) The same for HI ( $4d^{-1}$ ).

TABLE VII. Comparison between atomic estimations and molecular calculated values of the  $\bar{P}$  spin-polarization parameter for ionization from a  $d$  shell.

	Threshold energy		
	Atomic value	Molecular value	
	$p$ wave	HBr	HI
$\bar{P}_{\Pi_{1/2}}$	0.25 <sup>a</sup>	0.2	0.2
$\bar{P}_{\Delta_{3/2}}$	0.5 <sup>b</sup>	0.47	0.4
$\bar{P}_{3/2}$	0.3	0.23	0.2
	Resonance energy <sup>c</sup> $\epsilon_r$		
	$f$ wave		
$\bar{P}_{\Pi_{1/2}}$	-0.17 <sup>d</sup>	-0.15	-0.19
$\bar{P}_{\Delta_{3/2}}$	-0.33 <sup>e</sup>	-0.3	-0.3
$\bar{P}_{3/2}$	-0.15 <sup>f</sup>	-0.15	-0.16

<sup>a</sup>The  $p\sigma$  wave only contributes to the value of  $\bar{P}$  and the transition moments from a pure  $\pi nd$  orbital to pure  $\epsilon p\sigma$  and  $\epsilon p\pi$  orbitals are equal.

<sup>b</sup>The  $p\pi$  wave only contributes to the value of  $\bar{P}$ .

<sup>c</sup> $\epsilon_r = 3$  a.u. for HBr and 0.5 a.u. for HI.

<sup>d</sup>The transition moments from  $\pi nd$  to  $\epsilon f\sigma$ ,  $\epsilon f\pi$ , and  $\epsilon f\delta$  are in the ratio  $\sqrt{3}:2/\sqrt{2}:\sqrt{10}$ .

<sup>e</sup>The transition moments from  $\delta nd$  to  $\epsilon f\sigma$ ,  $\epsilon f\pi$ , and  $\epsilon f\delta$  are in the ratio  $\sqrt{6}:1:\sqrt{15}$ .

<sup>f</sup>The cross sections  $\sigma_{\Pi}$ ,  $\sigma_{\Delta}$ , and  $\sigma_{\Sigma}$  for a pure  $p$ - $d$  transition are in the ratio  $\frac{1}{5}:\frac{1}{5}:\frac{1}{7}$ .

polarization parameters have been calculated using Hund's coupling case (c) and their values for  $J_a^+ = \frac{3}{2}$  are given in Figs. 5(a) and 5(b) for HBr and HI, respectively. Their variation with energy compares well if one notes that the maximum in the cross section lies at much higher energy in HBr than in HI.

A comparison between the calculated values and those obtained in a pure atomic case is easy for the  $\bar{P}$  parameter and is given in Table VII. In this table  $\bar{P}_{3/2}$  is obtained as a mean value of  $\bar{P}_{\Pi_{1/2}}$  and  $\bar{P}_{\Delta_{3/2}}$  [Eq. (29a) where  $\beta$  is replaced by  $\bar{P}$ ].  $\bar{P}_{\Pi_{1/2}}$  is given by Eq. (31) and  $\bar{P}_{\Delta_{3/2}}$  is obtained from Eq. (19b) applied to a  $\Delta$  core as

$$\bar{P}_{\Delta_{3/2}} = \frac{1}{2} \sum_l (M_{\Delta_{3/2}}^{l,\pi\pi} - M_{\Delta_{3/2}}^{l,\phi\phi}) = \frac{1}{2\sigma_{\Delta}} (\sigma_{\Delta}^{\pi} - \sigma_{\Delta}^{\phi}). \quad (38)$$

The atomiclike values are obtained assuming pure atomiclike  $nd$  initial and  $\epsilon l$  final orbitals for the photoelectron ( $\epsilon p$  orbital close to threshold,  $\epsilon f$  orbital in the region of the maximum of the cross section). The molecular values contain the contributions of all the partial waves. It is clear that in the two regions studied, the  $l$  mixing is weak and the same partial wave ( $p$  or  $f$ ) dominates, in atom and in molecule.

In Figs. 6(a) and 6(b) the partial contributions to the parameters  $\gamma$  and  $\xi$  coming from the different  $\Pi$  and  $\Delta$  ionic cores have been plotted. The difference between these contributions can be understood by the inspection of Tables III and IV. For example, this explains why at the  $\epsilon_r$  value  $|\gamma_{\Delta_{3/2}}| > |\gamma_{\Pi_{1/2}}|$  in HI [see Fig. 6(a)]. Except close to the threshold, the dominant term in  $\gamma$  is always  $\gamma^{ff}$  [Fig. 7(a)]. In the case of a  $\Pi$  core, it is the  $\delta$

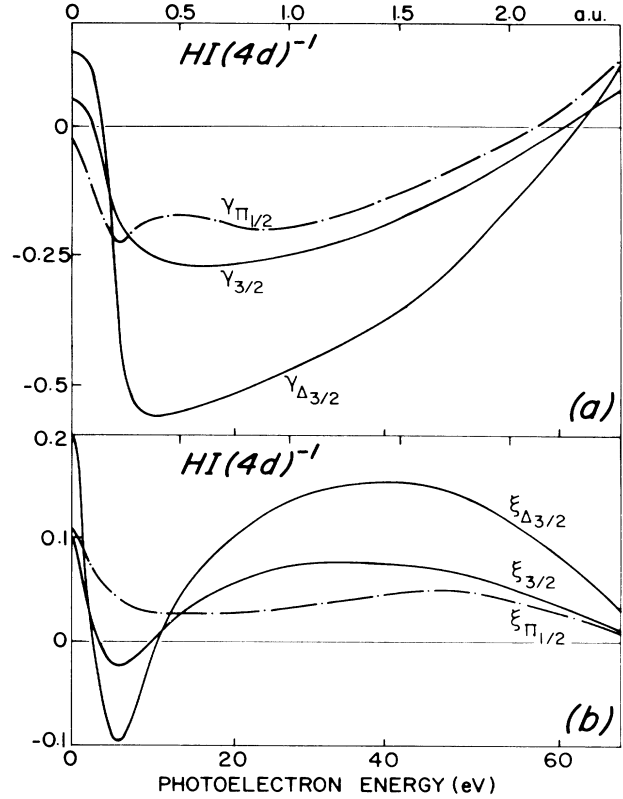


FIG. 6. (a) Details of the contributions of  $\gamma_{\Lambda^+ \Omega^+}$ , namely,  $\gamma_{\Pi_{1/2}}$  and  $\gamma_{\Delta_{3/2}}$  to  $\gamma_{J_a^+} = \gamma_{3/2}$  for HI ( $4d^{-1}$ ). (b) The same for  $\xi_{3/2}$ .

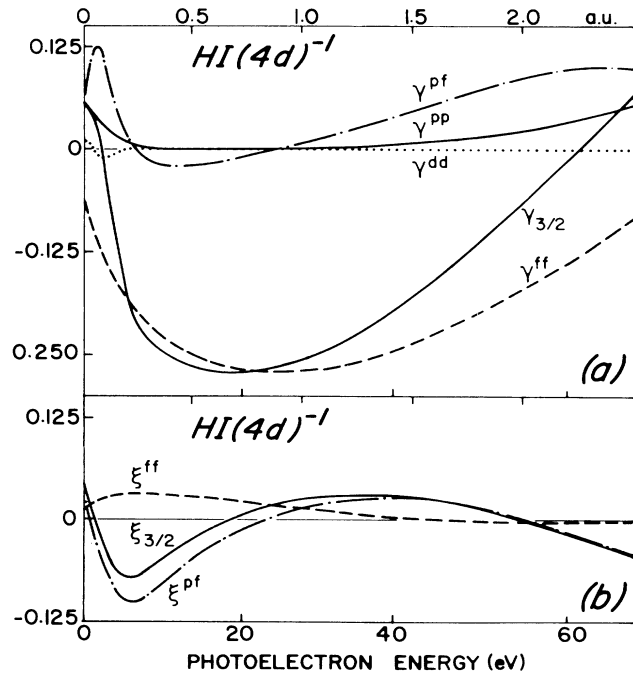


FIG. 7. (a) The different  $\gamma^{ll'}$  contributions for  $\gamma_{3/2}$  in HI ( $4d^{-1}$ ). (b) The different  $\xi^{ll'}$  contributions for  $\xi_{3/2}$  in HI ( $4d^{-1}$ ).

wave which has the most important contribution at  $\epsilon_7$  (see Figs. 2 and 3 of Ref. 31). Table III shows that  $\gamma_{\Pi}^{ff, \delta\delta} = 0$ . The calculated value of  $\gamma_{\Pi_{1/2}}$  is  $-0.17$  due to the nonzero  $\gamma_{\Pi_{1/2}}^{ff, \pi\delta}$  term. In the case of a  $\Delta$  core, the  $\phi$  wave has the largest contribution. From Table III,  $\gamma_{\Delta_{3/2}}^{ff, \phi\phi} = -0.33$ . The calculated value  $\gamma_{\Delta_{3/2}}^{ff}$  for HI is  $-0.49$ . The deviation from the total value of  $\gamma_{\Delta_{3/2}}$ , equal to  $-0.55$ , is due to the weak  $\gamma^{pp}$  and  $\gamma^{pf}$  contributions. The molecular-type contribution  $\gamma^{dd}$ , zero for the atomic case, is small at threshold and becomes negligible at higher energies. In the case of the  $\xi$  parameter, the atomiclike term  $\xi^{pf}$  is dominant [see Fig. 7(b)]. At low energy, there is a small contribution from  $\xi^{ff}$  which is a purely molecular effect and which vanishes completely at higher energies.

The energy variation of the spin-polarization parameters is roughly comparable to that of the corresponding atoms.<sup>11</sup> Unfortunately, the quantitative values of the molecular parameters are difficult to compare to the corresponding atomic values because we know<sup>31</sup> that for the  $d$  molecular inner-shell ionization where three ionic thresholds are degenerate, the static-exchange approximation does not always reproduce the experiments. We would like to compare our results with calculations made at a similar level of approximation for the iodine atom,<sup>44</sup> where multiple degenerate thresholds are also present, but the spin-polarization parameters have not been calculated in the one configuration approximation for this atom.

In this section, we have assumed that the ionic states corresponding to the ionization of the  $nd$  shell are in pure Hund's coupling case (c). To test this assumption, it would be interesting to measure the ratio of the two spin-polarization parameters with  $J_a^+ = 3/2$  and  $5/2$  at the same photoelectron energy. A ratio slightly less than  $-1.5$  [the theoretical value for Hund's case (c) Eq. (29b) with  $l'' = 2$ ] could indicate a tendency towards the Hund's case (a) for which a ratio of  $-1.0$  [Eq. (28b)] is obtained; however, other explanations are also possible.

#### IV. CONCLUSION

This work presents *ab initio* calculated values of the spin-polarization molecular parameters. The values obtained near the threshold for  $\xi$  in case of  $\pi np$  ionization compare well with the observed values at two energy points for  $\text{CH}_3\text{Br}$  and  $\text{CH}_3\text{I}$  (Ref. 45) but a more complete comparison with the experiment would be very useful. Experimental measurements for the  $\pi 5p$  ionization of HI are in progress at low energy,<sup>46</sup> where our results are the most valid. Unfortunately, the region above 40 eV where  $d$  ionization occurs is not accessible for the present experimental setup of the Heinzmann group.<sup>46</sup>

The molecular effects on the spin-polarization parameters seem difficult to identify out for the cases studied here which are atomiclike cases because they correspond to the ionization of nonbonding molecular orbitals. It would be interesting to perform experiments on molecules where the photoionization cross sections present a pronounced molecular character, for example, when molecular shape resonances appear in the continuum of an ion molecular state with  $\Lambda^+ \neq 0$ . Such an example could be AsO where a shape resonance is expected in the  $^3\Pi$  excited state of the ion as in NO.<sup>47</sup>

The predictions of  $\xi$  and  $\bar{P}$  for autoionizing resonances have been made recently<sup>5</sup> for HI and experiments are in progress.<sup>46</sup>

It would be easy to include vibrational motion in the present model but the vibrational effects would be difficult to observe in the hydrogen halides for which one vibrational peak is predominant in the photoelectron spectrum of the ion ground state. It would be interesting to study other molecules from this point of view.

Finally, an interesting extension would be the study of diatomic molecules oriented, for example, after dissociation of polyatomic molecules. The study of free oriented molecules is just beginning experimentally<sup>48</sup> and theoretically.<sup>49,50</sup>

<sup>1</sup>U. Heinzmann, F. Schäfers, and B. A. Hess, Chem. Phys. Lett. **69**, 284 (1980).

<sup>2</sup>U. Heinzmann, B. Osterheld, F. Schäfers, and G. Schönhense, J. Phys. B **14**, L79 (1981).

<sup>3</sup>G. Schönhense, V. Dzidzonou, S. Kaesdorf, and U. Heinzmann, Phys. Rev. Lett. **55**, 811 (1984).

<sup>4</sup>N. A. Cherepkov, J. Phys. B **14**, 2165 (1981).

<sup>5</sup>H. Lefebvre-Brion, A. Giusti-Suzor, and G. Rašeev, J. Chem. Phys. **83**, 1557 (1985).

<sup>6</sup>U. Fano, Phys. Rev. **178**, 131 (1969).

<sup>7</sup>N. A. Cherepkov, Adv. At. Mol. Phys. **19**, 395 (1983).

<sup>8</sup>U. Heinzmann, J. Phys. B **13**, 4353 (1980); **13**, 4367 (1980).

<sup>9</sup>F. Schäfers, G. Schönhense, and U. Heinzmann, Phys. Rev. A **28**, 802 (1983).

<sup>10</sup>N. A. Cherepkov, J. Phys. B **12**, 1279 (1979).

<sup>11</sup>K. N. Huang, W. R. Johnson, and K. T. Cheng, At. Data Nucl. Data Tables **26**, 33 (1981).

<sup>12</sup>G. Schönhense, F. Schäfers, U. Heinzmann, and J. Kessler,

Z. Phys. A **304**, 31 (1982).

<sup>13</sup>W. R. Johnson, V. Radojević, P. Deshmukh, and K. T. Cheng, Phys. Rev. A **25**, 337 (1982).

<sup>14</sup>F. Keller and F. Combet Farnoux, J. Phys. B **18**, 3581 (1985).

<sup>15</sup>K. N. Huang, Phys. Rev. A **22**, 223 (1980).

<sup>16</sup>N. A. Cherepkov, J. Phys. B **13**, L689 (1980).

<sup>17</sup>W. Thiel, Chem. Phys. **77**, 103 (1983).

<sup>18</sup>Ch. Heckenkamp, F. Schäfers, G. Schönhense, and U. Heinzmann, Z. Phys. D **2**, 257 (1986).

<sup>19</sup>U. Fano and D. Dill, Phys. Rev. A **6**, 185 (1972).

<sup>20</sup>D. Dill and J. L. Dehmer, J. Chem. Phys. **61**, 692 (1974).

<sup>21</sup>J. C. Tully, R. S. Berry, and B. J. Dalton, Phys. Rev. **176**, 95 (1968).

<sup>22</sup>M. E. Rose, *Elementary Theory of Angular Momentum* (Wiley, New York, 1957).

<sup>23</sup>C. M. Lee, Phys. Rev. A **10**, 1598 (1974).

<sup>24</sup>N. A. Cherepkov, J. Phys. B **14**, L73 (1981).

<sup>25</sup>J. Kessler, *Polarized Electrons* (Springer Verlag, Berlin, 1985).

- <sup>26</sup>P. O. Löwdin, *Phys. Rev.* **97**, 1474 (1955).
- <sup>27</sup>G. Raşeev and H. Le Rouzo, *Phys. Rev. A* **27**, 268 (1983).
- <sup>28</sup>G. Herzberg, *Molecular Spectra and Molecular Structures I Spectra of Diatomic Molecules* (Van Nostrand, Reinhold, Princeton, 1950).
- <sup>29</sup>H. Lefebvre-Brion and R. W. Field, *Perturbations in the Spectra of Diatomic Molecules* (Academic, Orlando, 1986).
- <sup>30</sup>H. Lefebvre-Brion, G. Raşeev, and H. Le Rouzo, *Chem. Phys. Lett.* **123**, 341 (1986).
- <sup>31</sup>F. Keller and H. Lefebvre-Brion, *Z. Phys. D* **4**, 15 (1986).
- <sup>32</sup>G. Raşeev, *Comput. Phys. Commun.* **20**, 267 (1980).
- <sup>33</sup>G. Raşeev, *Comput. Phys. Commun.* **20**, 275 (1980).
- <sup>34</sup>K. P. Huber and G. Herzberg, *Constants of Diatomic Molecules* (Van Nostrand, New York, 1979).
- <sup>35</sup>M. Mazzoni and M. Pettini, *Phys. Lett.* **85A**, 331 (1981).
- <sup>36</sup>M. Pettini, M. Mazzoni, and G. P. Tozzi, *Phys. Lett.* **82A**, 168 (1981).
- <sup>37</sup>H. Lefebvre-Brion, in *Giant Resonances in Atoms, Molecules and Solids*, NATO Advanced Study Institute, Series B (Plenum, New York, in press).
- <sup>38</sup>P. Morin and I. Nenner, *Phys. Rev. Lett.* **56**, 1913 (1986).
- <sup>39</sup>P. Morin and I. Nenner, *Phys. Scr.* **17**, 171 (1987).
- <sup>40</sup>T. A. Carlson, A. Fahlman, M. O. Krause, T. A. Whitley and F. A. Grimm, *J. Chem. Phys.* **81**, 5389 (1984).
- <sup>41</sup>C. E. Brion, Y. Iida, F. Carnovale, and J. P. Thomson, *Chem. Phys.* **98**, 327 (1985).
- <sup>42</sup>W. Thiel, *J. Electron Spectrosc.* **34**, 399 (1984).
- <sup>43</sup>T. A. Carlson, A. Fahlman, M. O. Krause, P. R. Keller, J. W. Taylor, T. A. Whitley, and F. A. Grimm, *J. Chem. Phys.* **80**, 3521 (1984).
- <sup>44</sup>F. Combet Farnoux and M. Ben Amar, *J. Electron Spectrosc.* **41**, 65 (1986).
- <sup>45</sup>G. Schönhense (private communication). Only the ratio  $\xi_{3/2}/\xi_{1/2}$  is given in Ref. 3.
- <sup>46</sup>N. Böwering, M. Müller, and U. Heinzmann, *Abstracts of the Fifteenth International Conference on the Physics of Electronic and Atomic Collisions, Brighton, 1987*, edited by J. Geddes, H. B. Gilbody, A. E. Kingston, C. J. Latimer, and H. J. R. Walters (ICPEAC, Brighton, 1987), p. 43; (private communication).
- <sup>47</sup>P. Morin, M. Y. Adam, P. Lablanquie, I. Nenner, M. J. Hubin-Frankskin, and J. L. Delwiche, in *Proceedings of the Seventh International Conference on VUV Radiation Physics, Jerusalem, 1983* (unpublished), p. 613.
- <sup>48</sup>S. Kaesdorf, G. Schönhense, and U. Heinzmann, *Phys. Rev. Lett.* **54**, 885 (1985).
- <sup>49</sup>N. A. Cherepkov, *J. Phys. B* **14**, L623 (1981).
- <sup>50</sup>N. A. Cherepkov and V. V. Kuznetsov, *J. Phys. B* **20**, L159 (1987).